

THESIS FOR THE DEGREE OF DOCTOR OF PHILOSOPHY

in

Machine and Vehicles Systems

**Thoracic injuries in frontal car crashes: risk  
assessment using a finite element human body model**

by

MANUEL MENDOZA VÁZQUEZ



Department of Applied Mechanics  
CHALMERS UNIVERSITY OF TECHNOLOGY  
Gothenburg, Sweden 2014

Thoracic injuries in frontal car crashes: risk assessment using a finite element human body model

MANUEL MENDOZA VÁZQUEZ

ISBN 978-91-7597-097-4

© MANUEL MENDOZA VÁZQUEZ, 2014.

Doktorsavhandlingar vid Chalmers tekniska högskola

Ny serie nr 3778

ISSN 0346-718X

Department of Applied Mechanics

Chalmers University of Technology

SE-412 96 Gothenburg

Sweden

Telephone + 46 (0)31-772 1000

Cover:

The modified THUMS in one of the impacts simulated in Paper III

Chalmers Reproservice

Gothenburg, Sweden 2014

Thoracic injuries in frontal car crashes: risk assessment using a finite element human body model

MANUEL MENDOZA VÁZQUEZ

Department of Applied Mechanics

Chalmers University of Technology

## **Abstract**

Accident data show that there is a clear need to improve the protection to occupants' thorax in frontal car crashes. For this purpose, models that can predict the risk of injuries and assess the occupant protection offered by different restraint systems are needed. Two types of models are usually applied to accomplish this, mechanical models, also known as anthropomorphic test devices (ATDs), and numerical models, of ATDs and of the human body. Numerical models of the human body based on the finite element method (FE-HBM) offer a more detailed representation of humans than ATDs. On the other hand, there is no clear consensus on the injury criteria and thresholds to predict thoracic injuries using FE-HBMs. The general aim of this thesis is to contribute to the reduction in number and severity of thoracic injuries in frontal car crashes by utilising an FE-HBM.

To reach this aim, the FE-HBM Total HUMAN Model for Safety version 3.0 (THUMS v3.0) was improved by comparing its kinematic and thoracic stiffness responses to tests with Post Mortem Human Subjects (PMHSs). Thoracic injury criteria at the global, structural and material levels were calculated with the modified THUMS in simulations of PMHS tests. Injury risk curves, with and without age adjustment, were constructed by applying the survival analysis method to matched pairs of injury criteria calculated with the modified THUMS and the injury outcome of the PMHS test. The injury risk curves that best approximated the test data were selected. Then, the risks predicted by the modified THUMS and the selected curves were compared to the risks predicted by an injury risk curve constructed based on real-world crash data. Different configurations of the modified THUMS were simulated and the results of the changes in the thoracic stiffness and coupling were applied to support the design update of the thorax of an existing ATD.

The contributions of this thesis include: modified THUMS, with an enhanced biofidelity in frontal car crashes compared to THUMS v3.0; injury risk curves for the modified THUMS to predict the risk of two or more fractured ribs in frontal car crashes; and recommendations to improve the design of an existing ATD thorax.

**Keywords:** Thoracic injury criteria; rib fracture; finite element; human body model; survival analysis; real-world crash data



## List of appended publications

This thesis is based on the work contained in the following papers, referred to by Roman numerals in the text:

- I. Mendoza-Vazquez, M., Brodin, K., Davidsson, J., Wismans, J., 2013. *Human rib response to different restraint systems in frontal impacts: A study using a human body model*. International Journal of Crashworthiness 18 (5), 516-529.
- II. Mendoza-Vazquez, M., Davidsson, J., Brodin, K., 2014. *Construction and evaluation of thoracic injury risk curves for a finite element human body model in frontal car crashes*. Submitted to Journal of Accident Prevention and Analysis, September 2014.
- III. Mendoza-Vazquez, M., Jakobsson, L., Davidsson, J., Brodin, K., Östmann, M., 2014. *Evaluation of thoracic injury criteria for THUMS finite element human body model using real-world accident data*. IRCOBI Conference, Sept 10-12. Berlin, Germany.
- IV. Brodin, K., Mendoza-Vazquez, M., Song, E., Lecuyer, E., Davidsson, J., 2012. *Design implications for improving an anthropometric test device based on human body simulations*. IRCOBI Conference, Sept 12-14. Dublin, Ireland.

## **Division of work**

- I. Mendoza-Vazquez planned the study, carried out the modelling work and analysed the results. Mendoza-Vazquez wrote the paper under the supervision of Brolin, Davidsson and Wismans.
- II. Mendoza-Vazquez planned the study, carried out the modelling work and analysed the results. Mendoza-Vazquez wrote the paper under the supervision of Davidsson and Brolin.
- III. Mendoza-Vazquez planned the study with contribution of the co-authors. Jakobsson carried out the accident data extraction and Mendoza-Vazquez carried out the statistical analysis of the data. Jakobsson and Östmann provided the vehicle interior model while Mendoza-Vazquez carried out the simulations and the subsequent analyses. Mendoza-Vazquez and Jakobsson wrote the paper with contributions by the co-authors.
- IV. Mendoza-Vazquez, Brolin and Davidsson planned the study. Mendoza-Vazquez executed the simulations with THUMS, and carried out the analysis of the results. Song and Lecuyer performed the analysis of the rib strain. The paper was written by Brolin with contributions by the co-authors.

## Table of Contents

Abstract.....	i
List of appended publications .....	iii
Division of work.....	iv
Preface .....	vii
Acknowledgements .....	viii
List of abbreviations and definitions.....	ix
1 Introduction .....	1
2 Aims .....	4
3 Anatomy.....	5
3.1 Thorax.....	5
3.2 Bone .....	6
4 Thoracic injury prediction.....	8
4.1 Thoracic injury mechanisms.....	8
4.1.1 Soft tissue injuries .....	9
4.1.2 Skeletal injuries .....	9
4.2 Factors affecting the risk of injury .....	11
4.3 Thoracic and rib injury criteria.....	12
4.3.1 Global level injury criteria .....	12
4.3.2 Structural level injury criteria .....	13
4.3.3 Material level injury criteria.....	13
4.4 Injury risk curve construction.....	14
4.4.1 Statistical methods to construct injury risk curves.....	15
5 Numerical models .....	19
5.1 THUMS .....	19
5.2 Thoracic injury assessment in human body models.....	26
6 Summary of papers .....	28
6.1 Summary Paper I .....	28
Summary of Paper II .....	29
Summary of Paper III.....	30
Summary of Paper IV.....	31

7	Injury predictability of different NFR2+ injury criteria using the modified THUMS: a comparison of ultimate strain with DcTHOR and shear stress.....	32
7.1	Aim .....	32
7.2	Method .....	32
7.3	Results.....	35
7.4	Discussion and conclusions .....	36
8	General discussion .....	38
8.1	Biofidelity .....	38
8.2	Rib loads .....	40
8.3	Injury risk curve construction.....	41
8.4	Risk comparison .....	42
8.5	Ultimate strain .....	44
8.6	Implications for human body models .....	44
8.7	Future work.....	45
9	Conclusions .....	47
	References .....	48
	Appendix A – Validation of a finite element Volvo V70 interior model .....	57
	Introduction .....	57
	Method .....	57
	Results .....	58
	Discussion and conclusions.....	60

Appended Papers I, II, III and IV

## **Preface**

The work presented in this thesis was carried out at the Injury Prevention Group, at the Vehicle Safety Division, Department of Applied Mechanics at Chalmers University of Technology under the supervision of Professor Jac Wismans, Associate Professor Karin Brodin and Associate Professor Johan Davidsson from 2009 to 2014.

The research was funded between 2009 and 2010 by the THORAX EU Project, between 2011 and 2012 by SAFER, the Vehicle and Traffic Safety Centre at Chalmers, and between 2013 and 2014 by the Strategic Vehicle Research and Innovation (FFI) programme at the Swedish Innovation Agency (VINNOVA). Project partners were Autoliv Research, Volvo Car Corporation, Volvo Group Trucks Technology, SAAB Automobile and Umeå University.

Parts of the simulations were performed on resources at Chalmers Centre for Computational Science and Engineering (C3SE) provided by the Swedish National Infrastructure for Computing (SNIC). Simulations for Paper III were carried out on resources provided by Volvo Group Trucks Technology. My working place has been the SAFER facilities in Gothenburg.

## Acknowledgements

The completion of this thesis has been possible thanks to the support of many people. I would like to express my gratitude to:

My supervisors Jac Wismans, Karin Brolin and Johan Davidsson for their guidance and encouragement; the industrial partners Lotta Jakobsson and Merete Östmann, Volvo Car Corporation, Bengt Pipkorn and Krystoffer Mroz, Autoliv Research, Fredrik Törnvall, Fredrik Jenefeldt, and Stefan Thorn, Volvo Group Trucks Technology, Mats Lindquist and Johan Iraeus, Umeå University.

Jeff Crandall, Richard Kent, Jason Forman and David Lessley from the University of Virginia for fruitful discussions at the beginning of my studies. Special thanks to Greg Shaw for sharing a bit of his experimental experience during my visit to the University of Virginia.

Dan Gustafsson, Volvo Car Corporation, for his assistance in the extraction of accident data and Linus Wågström, Volvo Car Corporation, for sharing his knowledge about acceleration pulses.

All my colleagues at Chalmers University of Technology and SAFER for contributing to a creative and inspiring working environment.

My master thesis students Ainhitze Mendizabal Dones, Gianfranco Ramirez and Jan-Frederik Rater.

Very many thanks to my parents Maria de las Misericordias and Manuel J. for making all this possible! And of course, thanks to my brothers Marcos and Moisés for standing by my side despite the distance!

Andrea for your love!

Manuel Mendoza Vázquez  
Göteborg, 14 November 2014

## List of abbreviations and definitions

50 <sup>th</sup> percentile male	Weight of 78 kg and height of 175 cm
3D	Three dimensions
AIC	Akaike Information Criterion
AIS	Abbreviated Injury Scale
ATD	Anthropomorphic Test Device or crash test dummy
CIREN database	Crash Injury Research and Engineering Network; an accident database in the United States including crash reconstruction and medical injury profiles
C <sub>max</sub> criterion	Maximum chest compression; a thoracic injury
DC criterion	Combined deflection criterion; a thoracic injury
DcTHOR	Combined deflection criterion for an updated THOR; a thoracic injury criterion
E	Elastic modulus
$\epsilon_{UT}$	Ultimate tensile strain
$\epsilon_{yield}$	Yield strain
EBS	Equivalent Barrier Speed
ECE	Economic Commission for Europe
FE	Finite Element
GHBMC	Global Human Body Models Consortium
HBM	Human Body Model, a numerical model of the human body
Hybrid III	A frontal anthropomorphic test device used for the evaluation of automotive restraint systems
IRC	Injury Risk Curve
LS-DYNA	An explicit and implicit finite element solver used in crash simulations
MAIS	Maximum Abbreviated Injury Scale
MB	Multi-body
NFR	Number of Fractured Ribs
PMHS	Post Mortem Human Subject
RadioSS	An explicit and implicit finite element solver used in crash simulations
ROC	Receiver Operating Characteristic
$\sigma_{UT}$	Ultimate tensile stress
$\sigma_{yield}$	Yield stress
T8	Eighth thoracic vertebra
THOR	Test device for Human Occupant Restraint; a frontal anthropomorphic test device

THUMS	Total HUman Model for Safety; a finite element human body model
US	The United States
VCmax	Maximum viscous criterion; a thoracic injury criterion
Contusion	A bruise, resulting from the damage to blood vessels
Costochondral joint	Joint between the ribs and the costal cartilage
Costovertebral joint	Joint between the ribs and the thoracic vertebrae
Laceration	A cut, resulting from tearing of soft body tissue
Pneumothorax	Abnormal collection of air or gas in the pleural space
Haemothorax	Collection of blood in the pleural space
Interpleural	Between the two layers of the pleura
Pleura	Membrane surrounding the lungs (visceral pleura) or lining the inner chest wall (parietal pleura)

# 1 Introduction

In 2013, the number of fatalities on the roads equalled approximately 1.24 million worldwide (World Health Organization 2013). For all fatalities worldwide, about 31% correspond to car occupants. The number of injured persons worldwide due to road injuries is more than 78 million persons needing medical care of which 9.2 million requiring hospital admission (Global Road Safety Facility; The World Bank; Institute for Health Metrics and Evaluation 2014). A review of fatal crashes in the US showed that about 50% of the drivers were killed in frontal crashes (Kent et al. 2005a). Cuerden et al. (2007) found that as many as 84% of all drivers killed in frontal crashes sustained at least a serious thoracic injury (AIS3+) according to the injury classification in the Abbreviated Injury Scale. Crandall et al. (2000) found that approximately 61% of all moderate and more severe (AIS2+) thoracic injuries were rib fractures and that the maximum thoracic AIS is defined by rib fractures for approximately 72% of the occupants sustaining a maximum thoracic AIS2+. The most common thoracic injury in frontal crashes is rib fractures as described by Carroll et al. (2010). Furthermore, Wanek et al. (2004) found that the number of rib fractures is a good indicator of other thoracic injuries.

The introduction of seat belts and air bags has contributed significantly to the decline in the number of fatalities and severe injuries in frontal crashes. Bean et al. (2009) estimated that the fatality risk for occupants wearing a seat belt in a vehicle fitted with air bags in frontal crashes is reduced by 61% compared to an occupant not wearing such restraints. Despite their introduction, the number of fatalities and injured occupants in frontal car crashes is still high. In 2007, in the US alone, 4,835 occupants sustained fatal thoracic injuries in frontal crashes although they were belted and an air bag deployed (Rudd et al. 2009). These data call for continuing the efforts in developing of improved vehicle restraint systems.

According to Haddon (1973) injuries occur when “energy is transferred in such ways and amounts, and at such rates, that animate structures are damaged”. In a crash, part of the kinetic energy of the restrained occupants is dissipated by the restraint systems, limiting the excursion of the occupants inside the car and reducing their relative velocity with respect to the car. Human response in a crash is studied with different human surrogates, such as volunteers, PMHSs and mechanical or numerical models. Since the loads involved can be injurious, the use of human volunteers is limited. PMHS tests are complicated and are only used for basic research. Therefore, tests using mechanical and numerical models are often used as human surrogates in the design and evaluation process of restraint systems since they are more repeatable and commonly less expensive than PMHS tests.

The use of human surrogates to evaluate restraint systems requires biofidelic models. Wismans (2005) defined biofidelity as the process of assessing a model's reliability against a set of PMHS tests or human volunteers. These tests must be relevant for the load cases of interest, in this case, frontal crashes with modern restraint systems such as seat belts and air bags.

Mechanical models of humans are also known as anthropomorphic test devices (ATDs). These are instrumented to measure acceleration, force, relative displacement, etc. The Hybrid III 50<sup>th</sup> percentile male is the most widely used ATD in the evaluation of restraint systems in frontal crashes. The Hybrid III is a regulated test device in the US Code of Federal Regulations and also in the European ECE Regulations. The Hybrid III is instrumented to measure the sternal displacement relative to the spine and the acceleration of the thorax centre of gravity (Foster et al. 1977). Another ATD suitable for frontal car crash tests is the THOR that has been under development since 1990 and is now close to finalisation. Some improvements with respect to the Hybrid III are the inclusion of ribs with humanlike inclination and shoulder-clavicle complexes to improve interaction with seat belts (Lemmen et al. 2013). In addition, the THOR has been fitted with thoracic instrumentation that allows for 3D measurement of the displacement of four points on the ribcage (Haffner et al. 2001).

Numerical models of humans are known as human body models (HBMs) and there are two main modelling methods; multi-body (MB) and finite element (FE). The MB method allows for calculating kinematic response (including global forces) by approximating the human body with rigid or deformable bodies with kinematic joints between them. The FE method allows calculation of kinematic, dynamic and material response, i.e., strains and stresses, by dividing the human body into small elements to approximate a solution for the governing differential equations. The MB method is usually preferred over FE when the objective is to study the kinematic and global dynamic response, since the MB method requires less computational time than the FE method. If the objective is to study the material response, as to study the stresses and strains in a rib, the FE method is the choice.

According to several regulations, Hybrid III is the ATD to use in the evaluation of restraint systems. The Hybrid III uses maximum chest compression, i.e., mid-sternum displacement with respect to the spine, and thoracic spine acceleration to evaluate restraint system performance in frontal crashes. These injury criteria, chest compression and acceleration, are related to the risk of thoracic injury through an injury risk curve. Less risk of injury implies a greater occupant protection. It has been found that the maximum chest compression assessed with Hybrid III is not sensitive to modern restraint systems (Petitjean et al. 2002). This is in part because of limitations with the ATDs and in part limitations with

the criterion. ATDs have shown non-biofidelic stiffness distributions on the thorax (Shaw et al. 2005), leading to non-biofidelic deformations of the rib cage. A limitation with the criterion is that chest compression is evaluated at the mid-sternum, with only one point it is difficult to capture the deformation of the thorax under asymmetric loads like the ones from seat belts (Song et al. 2011).

An advantage of the FE-HBMs over the ATDs is that the FE-HBMs offer a more detailed description of the human anatomy, potentially allowing studies of injury mechanisms even at tissue level (Wismans et al. 2005). Therefore, there are several physical parameters that can be measured and related to risk of injury. Chest compression, single rib deflections, stresses and strains on the ribs are some of these. At the moment a commonly accepted and available definition of thoracic injury criteria for FE-HBMs however has not been established yet and therefore the subject continues to be of interest as a research topic.

## **2 Aims**

The general aim of this thesis is to contribute to the reduction in number and severity of thoracic injuries in frontal car crashes by utilising an FE-HBM. To reach this general aim, three specific aims are defined. The first one is to assess the biofidelity of an FE-HBM and improve the model if the biofidelity is not satisfactory. The second is to construct and evaluate injury risk curves for an FE-HBM to predict the risk of two or more fractured ribs in frontal car crashes. The third is to support the development of an updated ATD.

### **3 Anatomy**

In this section, a brief description of the thorax anatomy is given, including a description of the composition and architecture of bone that supports and protects the thoracic organs.

#### **3.1 Thorax**

The thorax is composed of the ribcage, superficial tissues and contains the principal organs of respiration and circulation. The upper part of the thorax connects to the neck and shoulders. The clavicle and scapula bones are considered to be part of the shoulders. The lower boundary of the thorax is delimited by the diaphragm. The diaphragm is a thin flat muscle that separates thoracic organs from the abdominal organs. The ribcage, depicted in Figure 1, comprises twelve pairs of ribs, twelve thoracic vertebrae, rib cartilage, the sternum and all their corresponding joints. Ribs are numbered from one to twelve, starting with the rib closest to the neck. All ribs are joined posteriorly to their corresponding vertebrae through the costovertebral joints. The anterior part of the first seven pair of ribs is attached through costal cartilage to the sternum, forming the chondrosternal joints. Ribs eight to ten are indirectly attached to the sternum through costal cartilage and the seventh ribs. Ribs 11 to 12 are not attached anteriorly to any skeletal structure and are therefore called floating ribs. All ribs are connected by means of intercostal muscles between each rib. The vertebral discs are located between each vertebra. The following three regions are found inside the cavity of the ribcage:

- The mediastinum is limited by the sternum on the anterior side, by the thoracic vertebrae on the posterior face and the lungs on the sides. The mediastinum contains the heart, aorta, vena cava, pulmonary veins and arteries, oesophagus, trachea and nerves.
- The right and left lungs are the other two regions inside the ribcage; each lung is surrounded by a serous membrane named visceral pleura. The inner face of the ribcage is covered by a membrane called the parietal pleura. A permanent under-pressure between both the visceral and parietal pleura protects the lungs from deflation.

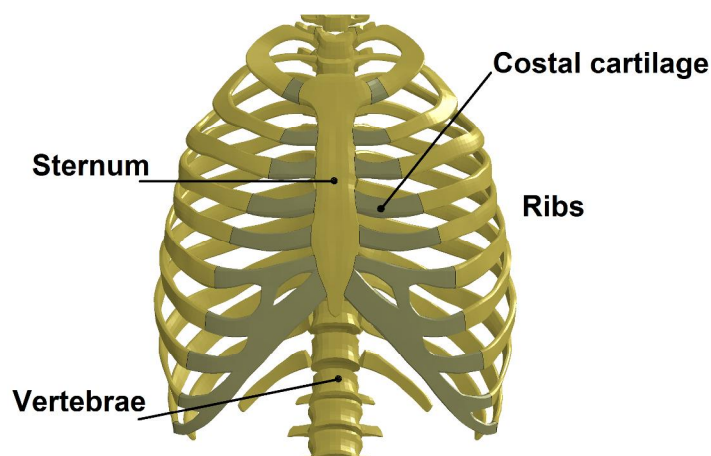


**Figure 1. The ribcage**

The ribcage, besides protecting and supporting the thoracic organs, is also involved in respiration. Respiration has two components, the abdominal and the thoracic. The abdominal component is performed by the diaphragm and abdominal muscles. Tensing the diaphragm instigates a downward movement and allows lung expansion. Exhalation occurs when the diaphragm relaxes and moves upwards. The thoracic component of respiration involves a change in the volume inside the ribcage, achieved thanks to the action of the intercostal muscles and the mobility of the ribcage at the costovertebral and chondrosternal joints.

### **3.2 Bone**

Bone is a multiphase material with a complex structure. It is composed of mineralised collagen fibres. It is the mineral salt, hydroxyapatite, that gives bone its stiffness, and collagen provides toughness to the bone (Turner 2006). The mineral and collagen fibres are arranged in two different architectures, the cortical (compact) and trabecular (cancellous), (Gomez et al. 2002) where the compact bone is more resistant to mechanical forces than the trabecular. In the cortical bone, the mineral and collagen fibres are organised into concentric lamellar groups around a central canal to form an osteon. The central canal, called the haversian canal, contains blood and lymph vessels. In the trabecular bone, the minerals and fibres are arranged in a trabeculae or lattice pattern. The cortical bone forms an outer shell, while the more porous trabecular bone fills the inner volume as shown in Figure 2.

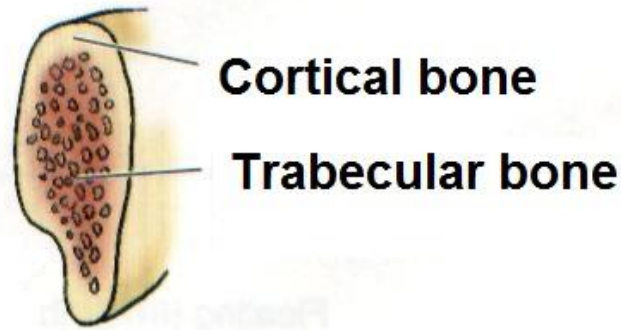


**Figure 2. Rib cortical and trabecular bone**

The mechanical properties of bone depend on its architecture and composition. Cortical bone, responsible for the majority of the strength of bone, is an anisotropic material and, as many biological materials, its mechanical response is rate sensitive. For example, the elastic modulus ( $E$ ) of bone along the longitudinal axis (femur shaft) can be 50% higher than the modulus along the transversal axis (Viano 1986) and (Hoffmeister et al. 2000). The elastic modulus increase when the strain rate increase, but an increase of an order of magnitude in the strain rate is needed before this effect is appreciable (Kent 2002). A description of the mechanical properties of human rib bone is given in Section 4.1.2.

## 4 Thoracic injury prediction

Thoracic injuries can be classified as blunt and penetrating. Blunt injuries arise when an object impacts the thorax without penetrating it. Penetrating injuries are not common in car crashes and have not been considered in this thesis. The injuries are classified as skeletal or soft tissue injuries. Thorax injuries can be rated according to the Abbreviated Injury Scale (AIS). Examples of thoracic injuries and their rating according to the AIS are presented in Table 1.

**Table 1 AIS for thoracic injuries (Association for the Advancement of Automotive Medicine 1998)**

AIS	Injury	Skeletal injury	Soft tissue injury
0	Non injured		
1	Minor	One rib fracture	Contusion of bronchus
2	Moderate	2 to 3 rib fractures, sternum fracture	Partial thickness bronchus tear
3	Serious	4 or more rib fractures on one side, 2-3 rib fractures with haemothorax or pneumothorax	Lung contusion, minor heart contusion
4	Severe	Flail chest, 4 or more rib fractures on each of two sides, 4 or more rib fractures with haemo or pneumothorax	Bilateral lung contusion, minor aortic laceration, major heart contusion
5	Critical	Bilateral flail chest	Major aortic laceration, lung laceration with tension pneumothorax
6	Maximal		Aortic laceration with haemorrhage not confined to mediastinum

### 4.1 Thoracic injury mechanisms

The injury mechanisms related to blunt injuries are: compression, viscous loading and inertia loading, or the combination of any of these mechanisms (Viano et al. 2000). Compression of the thorax can cause fractures in the ribcage and laceration of the internal organs. In this case, the elastic stiffness of the ribcage and internal organs withstand the compression until their material cannot accommodate more energy. Lung contusion is an example of injuries caused by viscous loadings. In this case, a potentially injurious pressure wave is transmitted from the chest wall into the lungs due to a high loading rate on the chest wall. The inertial loading of the heart is one of the mechanisms behind aorta lacerations. In this case, the differences in density make the heart and aorta move at different velocities, which generates loads between them.

#### **4.1.1 Soft tissue injuries**

Injuries to the lungs are the most common visceral thoracic injuries in frontal car crashes (Carroll 2009). Lung contusion occurs when a pressure wave, either with or without associated rib fractures, damages the capillary bed of the alveoli. Lung laceration and even perforations can be produced by fractured ribs. Al-Hassani et al. (2010) found, from studies of 310 blunt trauma patients, that the incidence of pulmonary contusion increases as the number of rib fractures increases. Carroll et al. (2010) reported from in-depth accident analysis that young occupants tended to receive AIS3+ lung injuries without receiving AIS3+ thoracic skeletal injuries, while older occupants tended to receive AIS3+ rib fractures alone or together with AIS3+ lung injuries. At the same time Carroll et al., in a case-by-case analysis, found that young occupants tended to receive only slight injuries in quite severe accidents while older occupants sustained severe injuries in relatively low crash severities. As stated in Section 1, Crandall et al. (2000) identified that the maximum thoracic AIS is defined by rib fractures in approximately 72% of the occupants sustaining a maximum thoracic AIS2+. Based on these findings, this thesis focuses on the prediction of rib fractures since rib fractures can imply fatal complications and are related to the magnitude of the overall thoracic trauma.

#### **4.1.2 Skeletal injuries**

When the loads in the bone material exceed the strength of the mineral salt or the collagen fibres, failure starts. Complete fracture represents the separation of the molecules that compose the microstructure of bone (Viano 1986).

Chest wall pain is involved in the majority of the complications of rib fractures; it limits the pulmonary function and the ability of patients to clear secretions, increasing the risk for pulmonary infections (Karmy-Jones et al. 2004). Other complications arise from displaced rib fractures, where the rib fragments can perforate the pleura and cause pneumothorax or haemothorax. During these states, the interpleural space is filled with air, pneumothorax, or blood, haemothorax, and the lungs begin to collapse. Multiple fractures can lead to thorax instability and flail chest. Flail chest occurs when a part of the anterior and/or lateral chest wall move freely. The part of the chest that has free movement, moves inward on inspiration and outward on expiration, diminishing ventilation.

Even if a low number of rib fractures is considered as a minor injury, patients might develop life-threatening complications up to approximately 72 hours post-injury (Battle et al. 2013). Battle et al. (2012) identified factors that increased the risk of mortality following blunt chest trauma. These factors include being aged 65 and above, three or more rib fractures, previous cardio-pulmonary disease and the development of pneumonia post-injury. To meet the Vision Zero

target where ultimately no one should be killed or seriously injured within the road transport system (Tingvall et al. 1999), it is critical to predict the second rib fracture since three or more rib fractures can produce life-threatening complications.

The compression of the thorax during blunt impact generates loads on the ribs that can potentially fracture them and it is therefore relevant to know the loads that they are subjected to. Vezin et al. (2009) tested four ribcages to characterise their 3D deformation. Vezin et al. (2009) applied the load on the sternum and followed the movement of marker triplets on ribs two, four, six and eight. In this way they found that ribs two to six deformed mainly in an anteroposterior direction, including a considerable flexion as well. These deformations imply a bending load along the mean fibre of the rib, i.e., the line that is obtained by joining the centroids of consecutive cross sections of the rib, and a torsion load around the mean fibre of the rib. Rib eight displayed a deformation on its own plane, with anteroposterior and transverse deformations as illustrated in Figure 3. This figure shows the un-deformed and deformed states of rib four and eight after a blunt impact to the sternum. All states are shown with respect to a local coordinate system on the corresponding rib, it is clear that rib four presents greater deformations out of the XY plane than rib eight. Duma et al. (2006) measured the strain on the parietal surface of the ribs of PMHSs on a table top belt loading device. They found that the first principal strain was not very far away from the longitudinal strain of the rib, the largest deviation between these strains was  $19.9^\circ$  on rib three. This deviation could also be explained by the superposition of bending and torsion loads on the ribs. Comparing the longitudinal and transversal strains on the ribs of an FE-HBM in different crash simulations, Song et al. (2011) found that the longitudinal strain was the main component compared to the transversal and concluded that the rib injury mechanism was bending. It is recognised that bending is one of the principal injury mechanisms behind rib fractures, but there is evidence that torsion is also involved. It is of interest to investigate if other mechanisms are involved as well, since they could influence which parameters to measure in order to predict rib fractures; e.g., measuring only the first principal strain or the first and second principal strains to predict injury fracture. This investigation was done in Paper I.

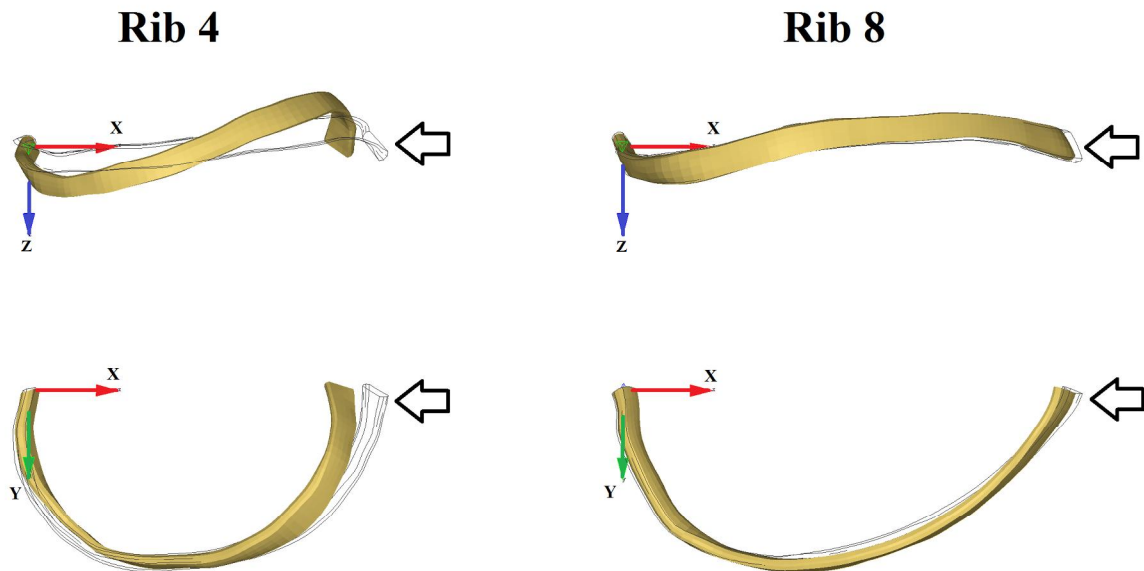


**Figure 3. Schematic description of the rib deformations under sternal loading**

#### **4.2 Factors affecting the risk of injury**

Accident data show that age is a factor that increases the risk of injury in frontal impacts (Stigson et al. 2012), particularly for thoracic injuries (Carter et al. 2014). The increased risk of injury is mainly due to the increased risk of rib fractures and accompanying intra-thoracic injuries (Carter et al. 2014). It is known that several physical changes occur with age, such as changes to the material properties of bones and cartilages, as described by Carter et al. (1978), Zioupos and Currey (1998) and Forman et al. (2014). According to Carter et al. (1978), the ultimate strain of rib cortical bone decreases by 5.1% per decade of life, based on an age reference group of 20-29 years. It has also been found that the ribcage geometry changes with age, as discussed by Kent et al. (2005b), who found that as we age ribs move closer to being positioned perpendicular to the spine. It is therefore of importance to include age as a factor in the prediction of rib fractures.

The size of the occupants has also been reported as a factor affecting thoracic injury (Cormier 2008) and (Carter et al. 2014). Both studies found that increasing body mass index (BMI) is associated with an increasing risk of thoracic injury, but this effect is less than that of age. In a series of PMHS tests, Kent et al. (2010) found a different kinematic response between obese and lean PMHSs. A delayed interaction between the bony structure and the seat belt in obese PMHSs was responsible of a longer hip excursion and less forward pitch motion, when compared to lean PMHSs. This kinematic response exposed the lower and more compliant part of the ribcage to loads from the seat belt, while

lean PMHSs pitched forward and the clavicle and upper part of the ribcage interacted with the seat belt.

Bose et al. (2011) reported a higher risk of injury for belted females than belted males in comparable crashes. Carter et al. (2014) found that females were more susceptible than males to thoracic injuries in frontal car crashes. A possible explanation is that females are generally seated closer to the steering wheel due to the average female being shorter in stature, decreasing the protection provided by standard restraint systems (Evans 2001) and (Bose et al. 2011). This might, however only be a partial explanation since the stature differences are consistent throughout adult life, although risks between the genders change with age (Carter et al. 2014). No clear difference in bone strength between young males and females has been identified; however hormonal changes reduce bone mineral density for aging females compared to males. This may imply that age could have a greater influence on female risk for rib fractures than for males (Kent 2002).

### **4.3 Thoracic and rib injury criteria**

Injury criteria establish a relationship between a function of physical parameters and a probability of injury to a specific body region. Several tests and analyses to obtain thoracic injury criteria for occupants in frontal car crashes have been conducted. Thoracic injury criteria can be classified into three different levels; the global, structural and material levels. Criteria based on a displacement, velocity, acceleration or force measured for the whole thorax is at the global level. At the structural level are the criteria measured at an individual organ, for example a rib. The criteria at the material level often involve the continuum description of the material behaviour, in this way stresses, strains, and internal energies can be used as injury criteria for a specific tissue, for example rib cortical bone.

#### **4.3.1 Global level injury criteria**

As described in Section 4.1, the injury mechanisms involved in thoracic injuries are compression, viscous loading and inertia loading, or their combinations. Thoracic criteria at the global level focuses on parameters related to these injury mechanisms. One of the pioneers on the study of thoracic injury criteria was Kroell et al. (1974) who impacted the mid sternum of several PMHSs with an impactor at different velocities and masses. These tests resembled the impact of the thorax with the steering wheel hub, a common impact for car drivers in the 60s and 70s, when seat belt use rates were low. Kroell et al. (1974) found that maximum chest compression ( $C_{max}$ ), defined as the maximum displacement of the sternum relative to the spine normalised relative to the initial thoracic depth, correlated better with the AIS score than impact force. Based on animal tests,

Viano (1986) proposed the maximum viscous criterion (VCmax) that combined the chest compression and chest compression rate to evaluate the risk for soft tissue injuries. Viano (1986) found the maximum viscous criterion as an effective predictor of soft tissue injuries for chest compression rates between 3 to 30 m/s. As the rate of seat belt use increased and airbags became more common, researchers focused on criteria sensitive to localised and asymmetric belt loads in combination with distributed airbag loads, and chest compression rates of approximately 1 m/s. The maximum chest deflection (Dmax) (Kleinberger et al. 1989) was proposed to capture localised deflections in the chest, as those from a belt, by taking the maximum deflection of five different points on the chest. Based on real-world data, Mertz et al. (1991) revised Cmax and proposed a new injury risk curve for this criterion. The combined deflection criterion (DC) (Song et al. 2011) and differential deflection criterion (DcTHOR) (Davidsson et al. 2014) were proposed to account for asymmetry in the compression of the thorax. All these criteria are based on global parameters measured on the thorax, parameters that are relatively easy to measure in a PMHS, ATD or HBM. On the other hand, due to the complex loading of the thorax during a frontal impact and since rib fracture is a phenomenon that occurs at the material level, a structural or material parameter measured on a rib or the rib cortical bone may be more suitable to predict rib fractures than a global criterion.

#### **4.3.2 Structural level injury criteria**

Measuring criteria at the structural level in a whole body PMHS test is complicated due to current instrumentation limitations. Therefore tests to measure these criteria include isolated human ribs. Charpail et al. (2005), Kindig (2009), and Li et al. (2010) have reported tests on human single ribs. In all these single rib tests, each end of the rib is attached to a mount that is allowed to freely rotate around an axis perpendicular to the rib plane. The mount for the posterior end is not allowed to translate, while the anterior mount is allowed to translate in the anteroposterior direction. In this way, the ribs were basically loaded in pure bending. The tests measured normalised displacement between the rib ends, force at the posterior end of the rib, and work applied to the rib until fracture.

#### **4.3.3 Material level injury criteria**

At the material level, three-point bending tests have been performed on a section of the rib or on the cortical bone. In the three-point bending tests, a straight section of the rib is simply supported on the visceral surface and a normal load to the parietal surface is applied at the mid-span of the specimen. Beam theory is usually applied to obtain the elastic modulus (E) and ultimate stress of a rib sample. Many of these beam theories assume that the rib sample is

homogeneous and isotropic. Therefore the elastic modulus obtained in these experiments represents an elastic modulus of a rib, and not specifically of the cortical nor trabecular bone.

Kemper et al. (2007) noted that three-point bending tests are limited by the need to introduce assumption or correction factors in order to calculate the elastic modulus (E) or the ultimate stress. Kemper et al. (2007) proposed that the ideal tests to determine mechanical properties of the rib cortical bone are tensile or compressive tests. In the tensile tests, small cortical bone coupons are machined from the ribs and tested. Results from tensile tests are reported in Table 2.

**Table 2 Material properties of human rib cortical bone from tensile tests**

Reference	E [GPa]	$\sigma_{\text{yield}}$ [MPa]	$\epsilon_{\text{yield}}$ [%]	$\sigma_{\text{UT}}$ [MPa]	$\epsilon_{\text{UT}}$ [%]
(Kemper et al. 2005)	13.9 $\pm 3.7$	93.9	0.88	124.2 $\pm 32$	2.71 $\pm 1.3$
(Kemper et al. 2007)	14.4 $\pm 3.1$	-	-	130.9 $\pm 22$	2.51 $\pm 1.1$
(Subit et al. 2011)	13.5 $\pm 2.6$	-	-	112 $\pm 24.5$	1.06 $\pm 0.29$

The differences in tensile ultimate strain between the tests may stem from two sources. The first one is that the PMHSs in the tests by Subit et al. (2011) were older than those in the tests by (Kemper et al. 2007). The second reason presented by Subit et al. (2011) is concerning differences in the experimental set up. It is possible that the clamps holding the bone coupon slipped off during the Kemper, et al. tests. Moreover, the cross section area of the bone coupons varied more in the tests by Kemper et al., compared to Subit et al., and how such variation influenced the measured strains is unknown (Subit et al. 2011).

#### 4.4 Injury risk curve construction

Different human surrogates ATDs, mathematical models of ATDs and HBMs are used in the design of restraint systems. The risk of injury assessed with these tools is commonly a design criterion for these systems. Usually, the risk of injury is found by measuring a physical parameter with any of the aforementioned human surrogates and looking for the corresponding risk according to an injury risk curve (IRC). To develop such IRCs, there is a need to define a physical parameter to be measured and to relate these parameters to the injury risk. To achieve the latter, the injury assessment samples, commonly PMHS tests or cases from real-world data with known injury outcome and crash severity, are replicated with ATDs or HBMs. Finally, the measurements from the human surrogates are matched with the samples injury outcome and an IRC is constructed according to a statistical method.

For the construction of IRCs, examples of injury assessment samples derived from both PMHS tests (Neathery 1974), (Hertz 1993) and (Kuppa et al. 2001), and real-world data (Mertz et al. 1991), (Eriksson et al. 2006) and (Kleiven 2007) were found in the literature. The boundary and initial conditions are well defined in the PMHS tests, but PMHSs are usually from elderly donors, lack active and passive musculature, as well as tissue lividity and autolysis being present (Kent et al. 2010). Horsch et al. (1991) noted that PMHSs sustained injuries more easily than car occupants at similar exposures. Foret-Bruno et al. (1978) found that tests with fresh PMHSs matching real world accidents overestimated the number of rib fractures by about three to five fractures. To account for the frailty in PMHSs, the IRC construction for an updated THOR considered a number of fractured ribs (NFR) equal or greater than five as an AIS2+ injury (Davidsson et al. 2014). In real-world data, on the contrary, car occupants are alive at the time of the crash; however the boundary and initial conditions are generally not well defined. Well defined boundary and initial conditions are necessary to replicate crashes with ATDs or HBMs. In this thesis, the PMHS test approach was followed to construct IRCs.

#### **4.4.1 Statistical methods to construct injury risk curves**

Several statistical methods for the construction of IRCs have been established. Among the most common methods applied to biomechanical data in the field of traffic safety are the Mertz/Weber method, certainty method, logistic regression, consistent threshold and survival analysis. A brief description of these methods is given below, beginning with an introduction of some definitions.

Censoring of biomechanical data, such as PMHS test results, can be left-censored, right-censored or exact (Vittinghoff et al. 2005). A data point is left-censored when injury is present after the subject has been exposed to a known stimulus. However, it remains unknown the exact stimulus (e.g. chest compression) level at which injury was sustained. A data point is right-censored when injury is not sustained and it is unknown how much more stimulus could be applied before injury occurs. A data point is exact when the injury occurs and the stimulus value is known at that moment.

Mertz et al. (1982) proposed the Mertz/Weber method to consider left and right censored tests. In this method, the construction of the IRC is based on an assumed statistical distribution and the injury criteria values of the strongest and weakest subjects. The strongest subject has the greatest injury criteria level and does not sustain an injury of interest during the test. The weakest subject sustains injuries of interest and registers the lowest injury criteria value. This method requires median ranking values to be assigned to the injury criteria values of the injurious tests in the range of the weakest and strongest subjects. Then, the IRC is constructed by fitting a normal distribution, as suggested by

Mertz et al. (1982), to the greatest and lowest median ranking values and corresponding injury criteria. The use of the strongest and weakest subjects to construct the IRC was supported by the assumption that these subjects would be closer to their individual injury threshold than any other subject in the sample. The accuracy of this method is limited by the difficulty to design an experiment to identify the weakest and strongest specimens.

The certainty method was introduced by Mertz et al. (1996). This method classifies the test results in two groups, certainty and uncertainty. In the certainty group are all tests that are known to be injurious or non-injurious for a prescribed level of stimulus. The uncertainty group includes the rest of the tests in the sample. The first step using this method is to identify the range of stimulus. This range starts with the lowest injurious stimulus level in the sample and ends with the greatest non-injurious stimulus. The second step is to divide the range of stimulus in a prescribed number of equal intervals. The third step is to generate the certainty group at each interval. At each interval, a right censored test is included in the certainty group as non-injurious as long as the stimulus interval values are less or equal to the test stimulus. When the test stimulus values are greater than the test value, the test is included in the uncertainty group. A left censored test belongs to the uncertainty group as long as the interval values are less than the test stimulus. When the interval values are equal or greater than the left censored test stimulus, the test is considered in the certainty group. The fourth step is to calculate the percentage of injurious tests for each certainty group at the different stimulus intervals. The points obtained in the previous step constitute the non-parametric IRC, a step function. Finally, the parametric IRC can be estimated from the non-parametric IRC. A limitation of this method is that the method discards information contained in the uncertainty group. At low levels of the injury risk criterion, the majority of the injurious tests are not considered. On the contrary, at the high levels of the injury risk criterion, the majority of the non-injurious tests are discarded. Consequently, the risk is underestimated at lower injury risk criterion values and overestimated at higher values of injury risk criterion.

Logistic regression models the relationship between a dichotomous dependent variable (injury or non-injury) and an explanatory variable, the injury risk criterion. Logistic regression can process left and right censored data. To estimate the coefficients of the logistic distribution defining this relationship, the maximum likelihood method is used. The maximum likelihood is based on finding the estimates which maximise the joint probability (likelihood) for the observed data under the chosen model (Vittinghoff et al. 2005). It is possible to consider more than one explanatory variable by using a multiple logistic regression approach. A disadvantage of the logistic regression method is that an

IRC that follows a logistic distribution gives injury risks greater than zero even if the injury criteria value is zero. As an example, for a zero maximum chest compression an injury risk of about 15% is predicted by the thoracic IRC in Eppinger et al. (1999).

The consistent threshold method was proposed by Nusholtz et al. (1999) for doubly censored data, where the tests are either left or right censored. This is a non-parametric maximum likelihood estimate method. Being non-parametric, the method does not require that the underlying distribution is known. The consistent threshold method is suitable to guide and support the choice of a particular distribution to be used in parametric methods. Kent et al. (2004b) found that IRCs constructed based on the consistent threshold method underestimate the injury risk at low stimulus levels and overestimates risk at the high end.

Survival analysis is a set of statistical methods for studying the occurrence and timing of events (Kleinbaum et al. 2012). These methods are commonly used in clinical studies to determine survival time, but the time variable can be replaced by other physical variables of interest. For example, time can be replaced by the bending moment applied to the human femur to study the occurrence of femur fractures, as presented by Kennedy et al. (2004). Survival analysis allows the use of censored and exact data. In the parametric survival analysis, it is common to use the Weibull, log-normal and log-logistic distributions. These distributions give IRCs with zero risk of injury at zero level of stimulus, which the logistic distribution does not. All three distributions are defined by two parameters and it is common to estimate these parameters using the maximum likelihood method.

Petitjean et al. (2011) compared the five aforementioned methods by performing statistical simulations on datasets derived from two predefined statistical distributions. They found that survival analysis lead to the lowest error in the statistical simulations and recommended this method for constructing IRCs based on biomechanical data. Survival analysis is also the method suggested by (International Organization for Standardization (ISO) 2014) for the construction of IRCs.

Kent (2002) listed two fundamental requirements and a desirable characteristic for an injury criterion or its corresponding IRC: it must be able to differentiate injurious from non-injurious loading conditions, and it must be with regards to the loading conditions of interest. A desirable characteristic is: the criterion or IRC should take into consideration occupant factors that affect the injury outcome. Additionally, Kent stated that it is desirable that the IRC is a continuous function to allow optimisation and cost-benefit calculations.

Parametric survival analysis gives continuous IRCs and allows the inclusion, in form of covariates, of occupant factors that affect the injury outcome. Survival analysis has advantages over other commonly used methods in biomechanics, as described in this Section. The IRC construction described in Paper II and Paper III is based on parametric survival analysis, considering the Weibull, log-normal and log-logistic distributions. The analyses were performed in R (R Core Team 2012) and the survival package in R by Therneau (2012).

Once the IRCs (statistical models) are constructed, it is time to compare them and select the IRC that better represent the experimental data. Since the experimental data are censored, it requires special methods to identify the statistical model that best represent the data. Here follows a brief description of these methods. The Akaike Information Criterion (AIC) was proposed by Akaike (1974) as a tool for selection of statistical models. The AIC is calculated based on the likelihood and the number of parameters in the statistical model. The lower AIC value, the better is the fit of the statistical model to the experimental data. This criterion is relative, in the sense that it is used to select a statistical model among several that describe the same dataset (Burnham et al. 2002). This criterion has been applied to the selection of IRCs in (Petitjean et al. 2012) and (Davidsson et al. 2014). The relative width of the 95% confidence interval has also been proposed (Petitjean et al. 2012) as a measure of IRC quality.

## 5 Numerical models

Several FE-HBMs representing the 50<sup>th</sup> percentile male have been developed in recent years in different FE codes. For example, the Human Model for Safety (HUMOS2), by Vezin et al. (2005) in the Radioss code and Total Human Model for Safety version 3.0 (THUMS v3.0, Toyota Central R&D Labs., Inc.) coded in LS-DYNA (Hallquist 2006). Holmqvist (2009) evaluated both models and found that THUMS v3.0 performed better than the HUMOS2 in impactor tests. Song et al. (2009) developed HUMOS2LAB based on HUMOS2. THUMS version 4.0 (Shigeta et al. 2009) was released a few years ago, incorporating improvements such as individual models of the thoracic internal organs. The Global Human Body Models Consortium (GHBMC) has recently released a 50<sup>th</sup> percentile male model (Gayzik et al. 2012) and (Vavalle et al. 2013b). This model contains approximately two million elements and the internal organs are individually modelled. The purpose of these models is to evaluate the occupant kinematics during a crash and to investigate injury mechanisms.

### 5.1 THUMS

The FE-HBM used in this study was THUMS v3.0. This model is coded and solved using the explicit LS-DYNA FE code. The explicit FE method finds its application in the solution of non-linear transient dynamic problems. The study of injury using FE-HBMs is an example of such problems. FE models require the definition of the material models. In the case of FE-HBMs, non-linear material models are required to characterise tissues such as bone, internal organs, etc. Large deformations of the FE-HBM during the crash also induce non-linearity. Since the loads are changing over time during a crash, the problem is transient dynamic.

THUMS v3.0 represents a 50<sup>th</sup> percentile male occupant, with a mass of 77 kg and stature of 1.75 m, aged between 30 and 40 years (Toyota Motor Corporation 2008). It roughly consists of 150,000 elements and 110,000 nodes. Bones are modelled using shell elements for the cortical bones and hexahedral elements for the trabecular bones, an approach that is common for all FE-HBMs mentioned in the previous paragraph. Joints are modelled anatomically including the major ligaments and bone to bone contact, no mechanical joints are included (Iwamoto et al. 2002).

The biofidelity of the thoracic response of different versions of THUMS has been evaluated in several publications. Oshita et al. (2002), with an early version of THUMS v1, and Kimpara et al. (2006), with a THUMS v1.52, compared the force-deflection response of the thorax to frontal and lateral pendulum impacts. Murakami et al. (2006) reproduced the table top tests by Kent et al. (2005c) and found that the agreement between the model and the PMHS results were

improved by changing properties in the rib cartilage. Pipkorn and Mroz (2009) compared THUMS v2.21 to PMHS sled tests and found that the chest compression measured with THUMS v2.21 was generally greater than that for the PMHSs. Pipkorn and Kent (2011) modified the mesh, as well as the material data and added muscles to the THUMS v2.21. Their model reacted similar to the PMHSs in the table top tests by Kent. In sum, numerous studies have been published on the subject of the thoracic biofidelity of THUMS; most report that modifications to the model are needed to improve its response. Furthermore, to the best of my knowledge, no publication has showed the thoracic response of any THUMS version to several load cases, i.e., sled and table top tests.

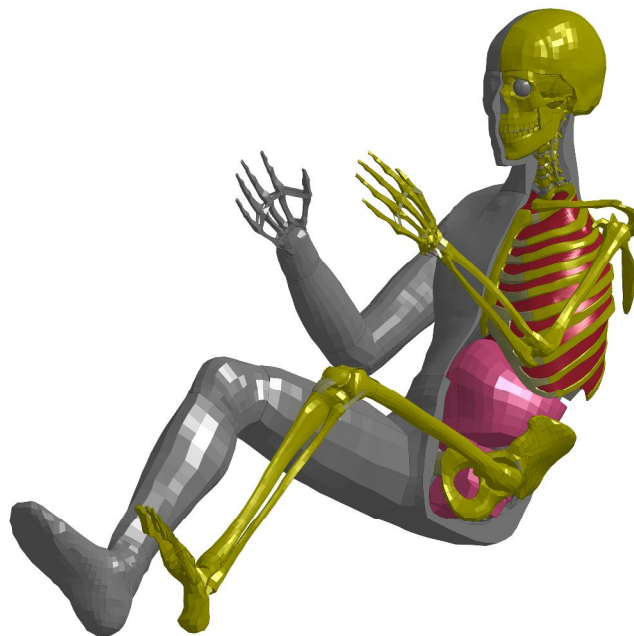


**Figure 4. Modified THUMS. Tissues were removed to make the skeleton and some internal organs visible**

Modifications and a biofidelity assessment of THUMS v3.0 have been carried out in this thesis, Paper I. These modifications to THUMS v3.0 resulted in the modified THUMS, shown in Figure 4. The modifications to THUMS v3.0 are listed below. Table 3 shows the number of elements and details concerning the modelling of the thorax for the modified THUMS, THUMS v3.0, THUMS v4.0, GHBMC and HUMOS2.

- A finer mesh of the ribs, intercostal muscles, rib cartilage, sternum and thoracic flesh, provided by Autoliv Research, was adapted to the THUMS v3.0, as shown in Figure 5.

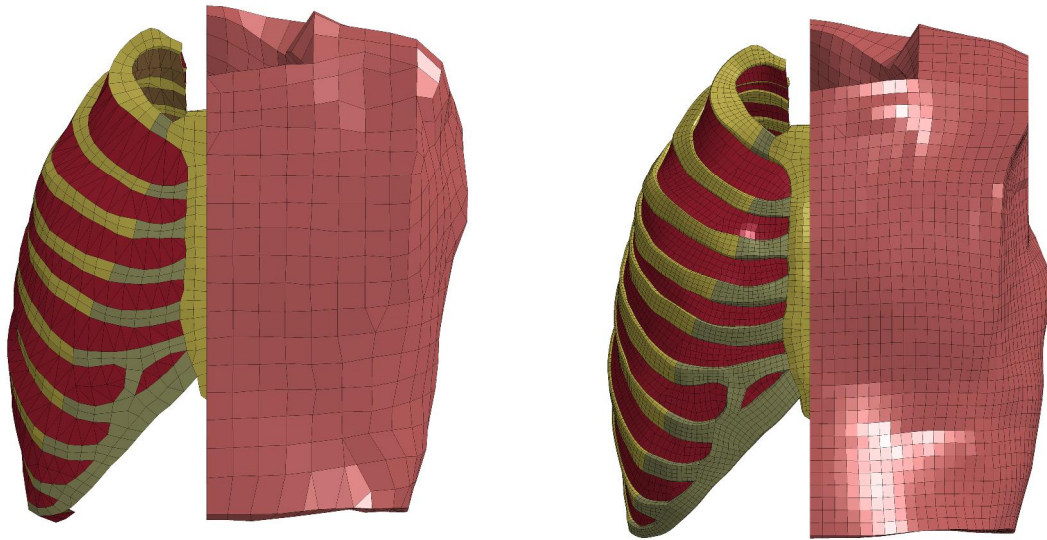


**Figure 5. THUMS ribcage for the original THUMS v3.0 (left) mesh and the finer (right) mesh**

- The element elimination option in all bones was deactivated. It was noted that once an element was eliminated, the simulations were likely to end prematurely due to numerical errors.
- The average cross sectional width of ribs seven and eight was adjusted according to data published by (Kindig 2009). Rib stiffness data from single rib tests by (Li et al. 2009) was used to compare the rib stiffness of the THUMS v3.0. Ribs seven and eight in THUMS v3.0 showed lower stiffness values than the experimental data and were therefore adjusted as described in Paper I.
- The stress-strain curve for the material of the volume representing the internal thoracic organs, in Figure 6, was modified according to the data published by Vawter et al. (1979) since the thoracic stiffness of THUMS, with the finer mesh, in table top tests was greater than the experimental values published by (Kent et al. 2005c). In these tests (Kent et al. 2005c) calculated the thoracic stiffness of the PMHSs in three different states, intact, denuded, and eviscerated. In the denuded state all superficial tissue to the ribcage was removed. In the eviscerated state all superficial tissue to the ribcage and internal viscera were removed. THUMS, with the finer mesh, showed a thoracic stiffness inside the range of the experimental values for the eviscerated state, but not for the other states. This motivated the change in material properties for the volume representing the internal thoracic organs.

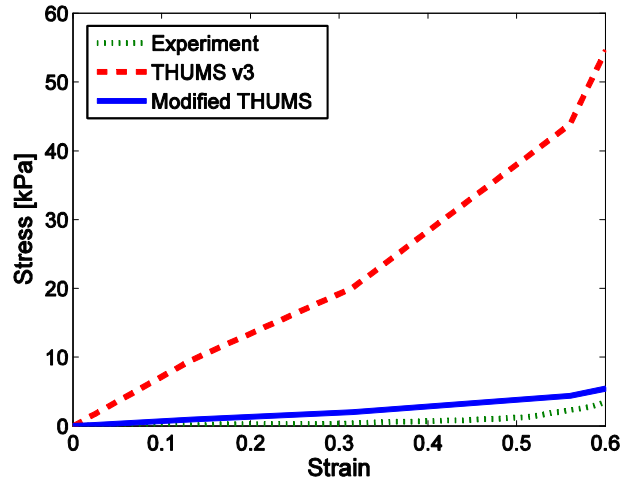


**Figure 6. Stress strain curves for the internal thoracic organs**

- The bulk modulus for the thoracic flesh was modified according to the data published by Ruan et al. (2003). This modification was also motivated by the results of THUMS, with the finer mesh, in table top tests by (Kent et al. 2005c).
- The rhomboid muscle was added to prevent excessive and unrealistic displacement of the scapula in sled tests, as described by Pipkorn et al. (2011).

The sagittal section of the thorax of the modified THUMS is shown in Figure 7. The thoracic internal organs are not represented individually; instead they are represented by a single volume of hexahedral elements. This volume is attached to the base of the neck and to the thoracic vertebrae. Around the complete volume there is a layer of shell elements that are constrained by contact to the ribcage, the intercostal muscles and the abdominal organs. The superficial tissues to the ribcage, i.e., skin, muscles and fat, are modelled as a volume of hexahedral elements attached to the base of the neck superficial tissues, to the top of the hip superficial tissues, and to the thoracic and lumbar vertebrae. This volume is also surrounded by shell elements restrained by contacts to the ribcage, intercostal muscles and abdominal organs.

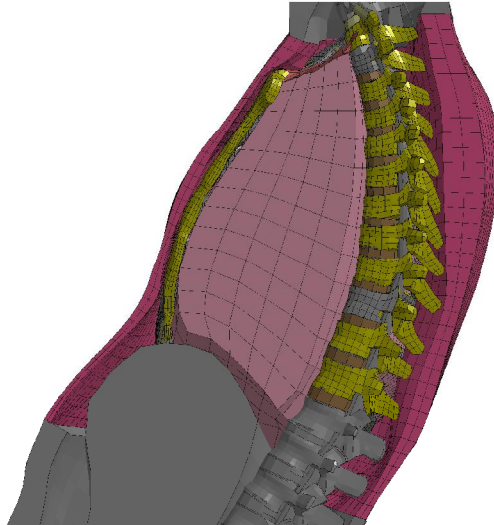


**Figure 7. Thorax of the modified THUMS, sagittal view**

The shell elements representing the rib cortical bone in the modified THUMS have a mean length of 3.5 mm, while the hexahedral elements have a mean length of 3.3 mm. Figure 8 shows a rib of the modified THUMS with the shell and hexahedral mesh. Li et al. (2010) reproduced single rib tests, where the ribs were compressed in the anteroposterior direction, and identified that rib models with a mean length of the hexahedral elements around 2 mm gave a good agreement between the experimental and simulated values of force and displacement at fracture. They also found that smaller element lengths marginally increased the model accuracy to predict the displacement and force at the time of fracture. As shown in Table 3, the GHBMC model is the model with the mean element length closest to 2 mm, with its 2.3 mm. The modified THUMS, with its 3.3 mm is the model that follows in mean element length.

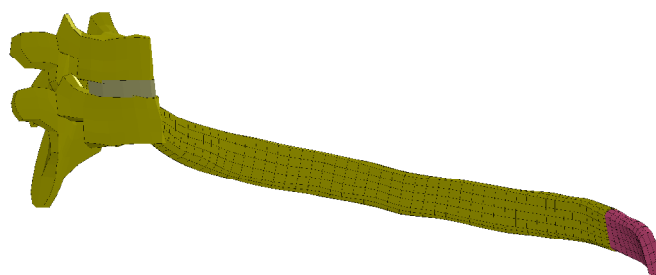


**Figure 8. Rib of the modified THUMS with its mesh, cortical (yellow) and trabecular (red) bone. Some elements of the cortical rib bone have been removed**

The cortical bone of the modified THUMS is modelled with a piecewise linear elasto-plastic model. The stress-strain curve for the material is depicted in Figure 9 along with the 95% confidence interval for the elastic modulus, the ultimate stress and ultimate strain obtained from tensile tests on coupons of

human rib cortical bone reported by Kemper et al. (2007). A curve corresponding to the stress-strain curve for a bone coupon test from the experiments by Kemper is also shown in Figure 9.

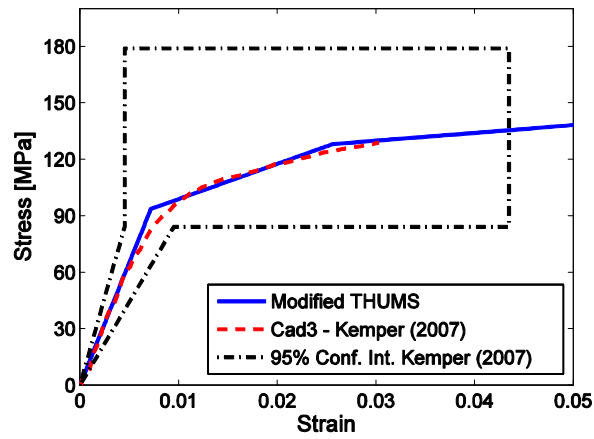


**Figure 9. Rib cortical bone stress-strain curve in the modified THUMS and experimental results**

**Table 3 Properties of the modified THUMS compared to different HBMs**

	Modified THUMS	THUMS v3.0	THUMS v4.0	GHBMC	HUMOS2
Reference	(Mendoza-Vazquez et al. 2013)	(Toyota Motor Corporation 2008)	(Shigeta et al. 2009)	(Gayzik et al. 2012)	(Vezin et al. 2005)
Solver	LS-DYNA	LS-DYNA	LS-DYNA	LS-DYNA	Radioss
Total Elements	209,769	143,052	1'713,828	2'184,928	70,393
Hexahedrals	90,822	65,545	1'312,977	1'663,647	21,542
Shells	115,508	74,100	395,024	515,252	47,244
Discrete/Beam	3,439	3,407	5,827	6,029	1,607
Shell elements	18,512	3,294	12,160	4,0724	5,284
Mean length	3.5 mm	8.4 mm	4.3 mm	2.2 mm	6.0 mm
Material model	PIECEWISE LINEAR PLASTICITY	PIECEWISE LINEAR PLASTICITY	PLASTICITY WITH DAMAGE	PIECEWISE LINEAR PLASTICITY	Elasto plastic
Elastic modulus	13 GPa	13 GPa	13.02 GPa	11.5 GPa	14 GPa
Yield stress	93.5 MPa	93.5 MPa	80 MPa	88 MPa	70 MPa
Density	2,000 kg/m <sup>3</sup>	2,000 kg/m <sup>3</sup>	2,000 kg/m <sup>3</sup>	2,000 kg/m <sup>3</sup>	6,000 kg/m <sup>3</sup>
Thickness	0.7 mm	0.7 mm	0.7 mm	Variable (nodal) 0.21-2.73 mm	Variable (regional) 0.5-1 mm
Element elimination	No element elimination	At 1.8% plastic strain	Damage starts at 2.0%. elimination at 50% plastic strain	At 2.0% plastic strain	At 4.0% plastic strain
Hexahedral elements	15,276	1,076	7,800	48,632	2,796
Mean length	3.3 mm	7.5 mm	4.2 mm	2.3 mm	5.9 mm
Material model	PIECEWISE LINEAR PLASTICITY	PIECEWISE LINEAR PLASTICITY	DAMAGE 2	PIECEWISE LINEAR PLASTICITY	Elastic
Elastic modulus	40 MPa	40 MPa	40 MPa	40 MPa	50 MPa
Yield stress	1.8 MPa	1.8 MPa	1.8 MPa	1.8 MPa	-
Density	862 kg/m <sup>3</sup>	862 kg/m <sup>3</sup>	862 kg/m <sup>3</sup>	1,000 kg/m <sup>3</sup>	1,000 kg/m <sup>3</sup>
Thoracic internal organs	One volume for thoracic organs	One volume for thoracic organs	Organs modelled individually	Organs modelled individually	Organs modelled individually

## 5.2 Thoracic injury assessment in human body models

The injury criteria at the global level described in Section 4.3 is usually measured with the Hybrid III or the THOR. Both ATDs are designed for frontal impact tests. To measure chest deflection, Hybrid III has one transducer attached to the sternum at one end and to its rigid spine at the other. THOR is instrumented to measure the ribcage deflection at four different points, between the ends of its third and sixth ribs, and a rigid section of the spine. With regards to THUMS and other FE-HBMs, their thoracic spine contains 12 vertebrae that can move with respect to each other and the ribcage contains hundreds of nodes that are traceable. Fortunately, a coordinate system attached at the eighth thoracic vertebra (T8) can be used as a reference to measure the ribcage deflection as in Shaw et al. (2009a) and Song et al. (2011). Once the coordinate system is defined in THUMS, as shown in Figure 10, nodes at the mid-sternum and rib ends can be tracked and used to describe ribcage deflections.

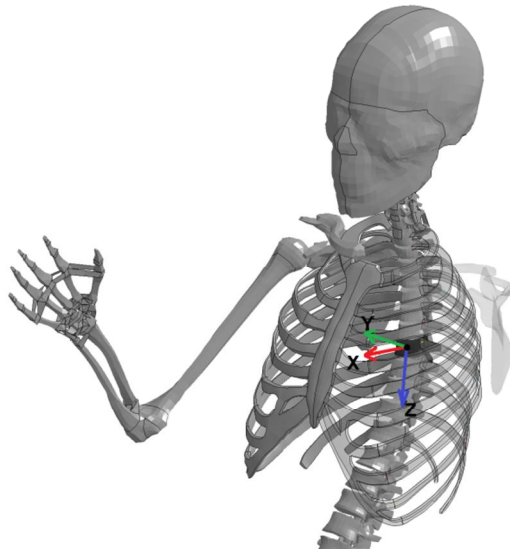


**Figure 10. Coordinate system at the eighth thoracic vertebra (T8)**

The injury criteria at the structural and material levels can easily be extracted from an FE-HBM. An FE-HBM was instrumented, as described by Song et al. (2011), to measure the deflection of its ribs, but the individual rib deflections were not used to predict injury. There are several methods to predict injury with criteria at the material level using FE-HBMs. One approach includes the elimination or softening of the rib elements when their plastic strain reaches a specific threshold value. The element elimination involves the deletion of the element from the model. The softening involves a decrease in the stress values while strains increase. In these approaches, the NFR is given by the number of ribs where elements have been eliminated or softened, as described by Iwamoto et al. (2002), Kent et al. (2005b), Song et al. (2011), Kitagawa et al. (2013), and Golman et al. (2014). Another approach has been proposed by Forman et al.

(2012), where the probability of sustaining an NFR is given based on the rib cortical bone strain outputs of an FE-HBM, results from human rib cortical bone tensile tests, and an assumed age of the model. A brief description of this method is provided in Section 7.

The FE-HBMs that use element elimination or softening are deterministic models, in the sense that an exact NFR is predicted given a single configuration and occupant characteristics, as in Kitagawa et al. (2013). To account for age in the prediction of NFR using element elimination or softening, one simulation per age is required, as in Song et al. (2011). As the aim of this thesis is to predict the risk of two or more fractured ribs, the element elimination approach would only give a binary (injury or non-injury) response, instead of the desirable continuous response described in Section 4.4. The method proposed by Forman et al. (2012) gives the probability of injury and accounts for age without the need of several simulations. This method would give a continuous response. However, the difficulties and uncertainties in machining and testing human rib cortical bone in tensile tests, and the variation in ultimate tensile strain reported in Section 4.3.3 made this thesis having to follow an IRC construction method based on matched simulations and PMHS tests.

## 6 Summary of papers

Brief summaries of the publications that support this thesis are given in this Section. The full papers are appended at the end of this thesis.

### 6.1 Summary Paper I

The first aim of Paper I was to present the biofidelity assessment of THUMS v3.0 in frontal car crashes. The second aim was to use THUMS to study the individual rib responses in different load cases representative of frontal car crashes. The biofidelity of THUMS v3.0 was evaluated by comparing its kinematic and thoracic stiffness responses to those from PMHS tests representative of frontal car crashes. Ribs forces, deformations and strains were used to study individual rib responses.

The results showed that the biofidelity of THUMS v3.0 was not satisfactory. Finer meshes in the ribcage and in the soft tissues around the ribcage were the most relevant modifications made to THUMS v3.0 to improve numerical robustness and stability. To improve its biofidelity and based on published data, softer material properties were defined to the volume representing the thoracic organs and the soft tissues superficial to the ribcage. In Figure 11, the force-chest compression responses of the modified THUMS and THUMS v3.0 with just a refined mesh (THUMS v3-R) are compared to the experimental corridor from impactor tests.

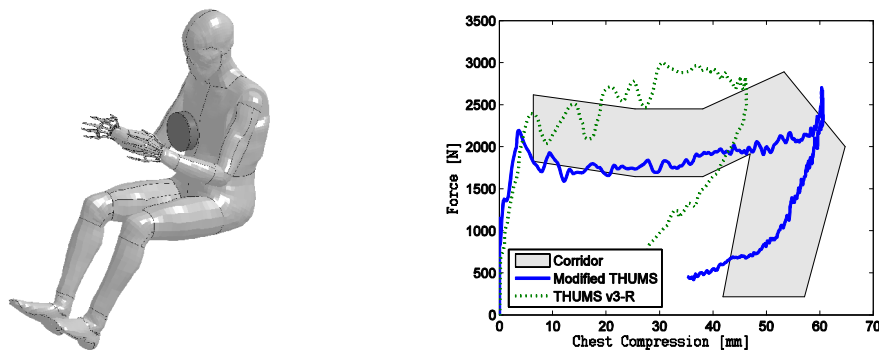


**Figure 11. The modified THUMS in an impactor test (left) and force-chest compression response (right) in the impactor test**

The results of the rib response to different load cases showed that ribs in the modified THUMS were subjected to bending, torsion and shear. A rib fracture criteria should be sensitive to these loads. Therefore, for criteria at the material level, a criterion that considers all principal strains or stresses appears to have better opportunities to predict rib fracture than only considering the first principal strain or stress. At the rib structural level, the preferred option appears to be a criterion that includes the out of plane displacement of the rib and not just the in plane displacement, i.e., anteroposterior compression.

## Summary of Paper II

The aim of this paper was to recommend a set of IRCs for the modified THUMS to predict rib fractures in frontal car crashes. Twenty-three PMHS tests were simulated with the modified THUMS. These tests included impactor tests reported by Nahum et al. (1970), Kroell et al. (1974) and Bouquet et al. (1994); table top tests by Kent et al. (2004a) and sled tests by Shaw et al. (2009b). Fourteen thoracic injury criteria at the material, structural and global levels were extracted from the modified THUMS in each simulated test. The values of these injury criteria were then matched with the injury outcome of the corresponding PMHS test. A PMHS with two or more fractured ribs was considered injured, while PMHSs with less than two fractured ribs were considered uninjured. Survival analysis was applied to the pairs of injury criterion values and injury/non-injury data to construct the IRC for each criterion. A second set of IRCs were constructed by including the PMHSs age at time of death as a covariate in the survival analysis to obtain age-adjusted IRCs. The Akaike Information Criterion (AIC) and the relative width of the 95% confidence interval were computed for each IRC and compared to identify the curves with the best performance. A parametric study was implemented to detect any sensitivity of the different criteria and corresponding IRC to changes to the restraint positions and material properties of the rib cortical bone.

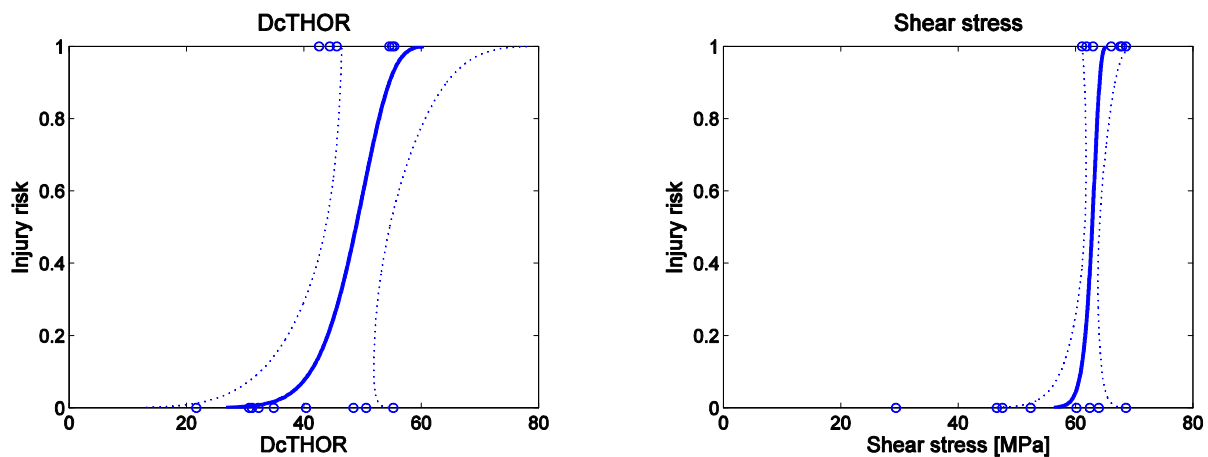


**Figure 12. Age-adjusted IRCs for DcTHOR and shear stress criteria**

The results showed that, among the evaluated IRCs, the age-adjusted IRCs shown in Figure 12 were the curves that performed best based on their AIC values and their confidence intervals relative width. No criterion at the structural level reached acceptable performance. It was found that the curve for DcTHOR was less sensitive to changes of the restraint positions and material properties of the rib cortical bone than the curve for shear stress.

### Summary of Paper III

The aim of this paper was to compare the thoracic injury risk predicted by the modified THUMS with the risks predicted by an IRC constructed based on real-world data. Since the IRCs for the modified THUMS were developed from reconstruction of PMHS tests, it is of interest to investigate their response in real-world crashes. For this purpose and applying survival analysis, a thoracic AIS2+ injury risk curve was constructed based on selected and representative frontal car crashes from the Volvo Cars' Traffic Statistical Accident Database. Then, the modified THUMS was positioned in a detailed and representative interior vehicle model of the selected cars from the database. Six simulations, with three different crash severities and two acceleration pulses for each severity, were performed with the modified THUMS in the interior vehicle model. The injury criteria Dmax, DcTHOR, shear stress and first principal strain in the ribs were computed with the modified THUMS for each of these six simulations. Then, the risks and their 95% confidence intervals were obtained from the IRCs constructed in Paper II. These risks were then compared to the risk from the real-world data, as shown in Figure 13.

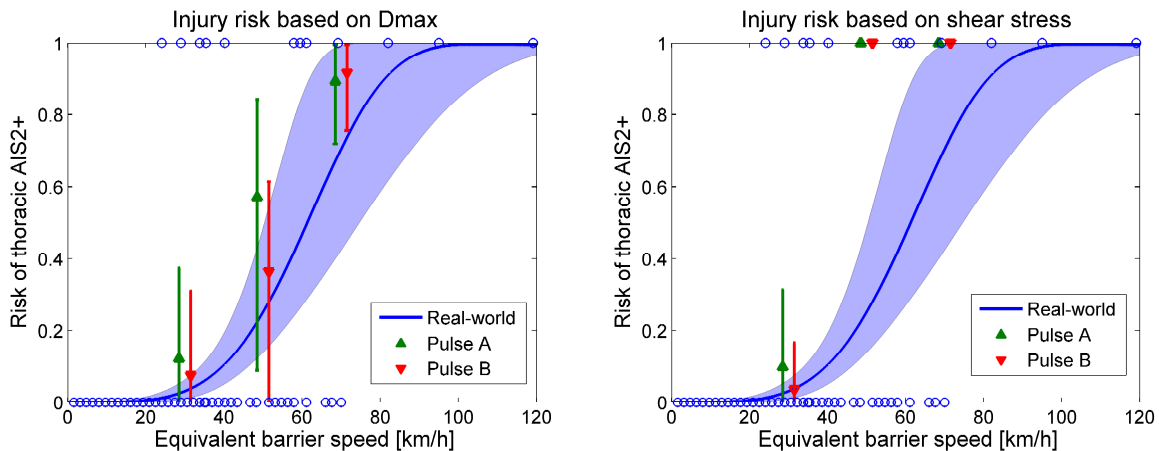


**Figure 13. Injury risk predicted by Dmax (left) and shear stress (right) strain and the modified THUMS at three EBS values and two acceleration pulses compared to the real-world data IRC**

The results showed that all four THUMS criteria predict higher risk compared to the risk predicted by the real-world injury risk curve. The risks estimated with Dmax were closest to the risk estimated by the injury risk curve based on real-world data. The risks predicted by the shear stress criterion were close to the risks from real-world data at an equivalent barrier speed of 30 km/h.

## Summary of Paper IV

The aim of this paper was to make recommendations to support the design update of an ATD thorax. This was achieved by introducing ATD-like simplifications into THUMS and estimating their influence on the thoracic response. The thoracic effective stiffness, coupling and chest deflection were the parameters used to characterise the thoracic response. These parameters were evaluated using THUMS in simulations of the table top tests by Kent et al. (2004a), and sled tests by Shaw et al. (2009b). The table top tests included loads from a hub, a belt, a double belt and a band. The first part of the study analysed the influence on effective stiffness and coupling by increasing the compliance of different thoracic tissues and organs. In the second part of the study, different simplifications present in THOR with respect to the human thorax were introduced in THUMS and their influence on the thoracic response was analysed.

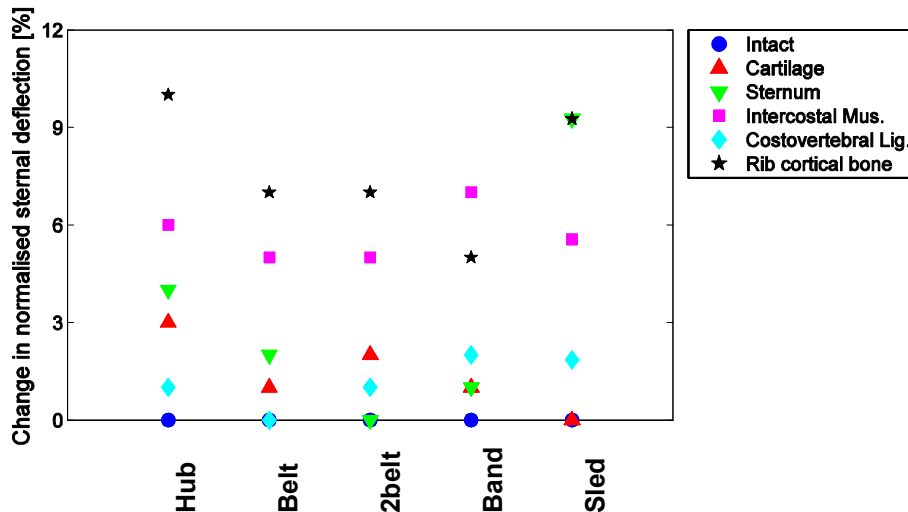


**Figure 14. Normalised sternal deflection for the THUMS in four table top tests and one sled test**

The results of the first part of the study showed that, for all tests, the rib cortical bone and the intercostal muscles had the greatest effect on chest deflections, as shown in Figure 14. Reducing the compliance of the rib cartilage and costovertebral ligaments displayed the least change in thoracic stiffness and chest deflections.

From the simulations it was concluded that an increase in rib stiffness is followed by an increase in thoracic coupling. Based on this conclusion, recommendations made to improve the design of THOR were to decrease the rib stiffness and include a spring-damper mechanism between the spine box and the rib anterior end to represent the stiffness of the thoracic organs.

## **7 Injury predictability of different NFR2+ injury criteria using the modified THUMS: a comparison of ultimate strain with DcTHOR and shear stress**

A method to calculate the risk of fractured ribs based on the rib cortical bone ultimate strain has been proposed by Forman et al. (2012). This method, referred in this thesis as the ultimate strain method, uses an age adjusted ultimate strain distribution, obtained from human rib bone tensile tests (Kemper et al. 2005, Kemper et al. 2007) to estimate local rib fracture probabilities with a THUMS 50<sup>th</sup> percentile male including in-house modifications. It is of interest to apply this method to the modified THUMS described in this thesis and compare the risks predicted with the ultimate strain method and the IRCs constructed in this thesis.

### **7.1 Aim**

The aim of this study is to compare injury predictability of the IRCs with age adjustment for the DcTHOR and shear stress developed in Paper II with the injury predictability of the ultimate strain method described by Forman et al. (2012).

### **7.2 Method**

The comparison was performed using the impactor, table top and sled tests described in Paper II. The risks for DcTHOR and shear stress were calculated based on the modified THUMS results in the simulations of the tests described in Paper II and the age adjusted IRCs obtained in Paper II. The parameters for these IRCs are presented in Table 4 for a Weibull distribution (Eq. 1). This distribution was the distribution suggested in Paper II for these criteria.

**Table 4. Distribution and parameters for the age adjusted curves**

<b>Criterion</b>	<b>Distribution</b>	<b>Intercept</b>	<b>Age coefficient</b>	<b>Log scale</b>
DcTHOR	Weibull	4.618	-0.011	-2.388
Shear stress	Weibull	4.338	-0.003	-4.096

$$Risk_{NFR2+} = CDF_{Weibull} = 1 - e^{-\left(\frac{x}{\lambda}\right)^\kappa} \quad \forall x \geq 0 ; 0 \forall x < 0 \quad \text{Eq. 1}$$

Where:

$CDF_{Weibull}$  is the cumulative distribution function for a Weibull distribution and is equal to the risk of NFR2+

$x$  is the injury criterion

$\lambda$  is the scale parameter, calculated as in Eq. 2

$\kappa$  is the shape parameter, calculated as in Eq. 3

$$\lambda = e^{age \cdot AC + I} \quad \text{Eq. 2}$$

Where:

$age$  is the age of interest, in years

$AC$  is the age coefficient from Table 4

$I$  is the intercept value from Table 4

$$\kappa = \frac{1}{e^{LS}} \quad \text{Eq. 3}$$

Where:

$LS$  is the log scale value from Table 4

For the ultimate strain, the greatest first principal strain for each rib was extracted and compared to the age adjusted ultimate strain value for each rib to obtain their fracture probabilities. These probabilities were then combined in a generalised binomial distribution to obtain the probability of NFR equalling a certain number. Since NFR2+ is the injury level of interest, the probabilities of zero and one NFR were computed, added and then their probability compliment calculated. It is this probability compliment that represents the risk of NFR2+ for the ultimate strain. For further details of this method, please refer to Forman et al. (2012).

The injury predictability comparison was performed as follows. A contingency table containing the true positives and negatives, and the false positives and negatives obtained with each injury criterion (DcTHOR, shear stress and ultimate strain) was generated. A true positive is when the criterion for the modified THUMS predicted an injury and the outcome of the test was injurious, while a true negative is when the criterion for the modified THUMS does not predict an injury and there is no injury in the corresponding test. The false positive case is when the criterion for the modified THUMS predicts an injury,

but there is no injury in the corresponding test. The false negative is when the criterion for the modified THUMS does not predict an injury, despite the corresponding test being injurious. A simulation with the modified THUMS was considered to predict an injurious outcome if the injury criterion yielded a NFR2+ risk equal or greater than 50%. A test was considered injurious if the NFR was equal or greater than two. An optimal injury risk criterion would identify all true positives and no false positives.

It is also of interest to know how the criteria classify the simulated tests as injurious or non-injurious while varying the threshold of the NFR2+ risk that defines injury. For that reason contingency tables were created for thresholds varying between 0% and 100%. These tables were the input to draw a receiver operating characteristic (ROC) curve for each injury criterion. In a ROC curve, the true positive rate is plotted on the ordinates and the false positive rate on the abscissas. In this case, the optimal injury risk criterion would have a rate of true positives equal to one and a rate of false positives equal to zero.

### 7.3 Results

Table 5 shows the risks predicted by the DcTHOR, shear stress and ultimate strain criteria, along with the age of each PMHS at time of death, as well as the NFR.

**Table 5. Risks for NFR2+ predicted by DcTHOR, shear stress and ultimate strain**

Test	PMHS	Reference	Age	NFR	Risk of NFR2+		
					DcTHOR	Shear stress	Ultimate strain
55	09FM	(Nahum <i>et al.</i> 1970)	73	0	0.32	0.39	0.46
60	11FF	(Kroell <i>et al.</i> 1971)	60	6	0.91	0.99	0.98
76	18FM		78	11	0.99	1.00	1.00
79	20FM		29	0	0.05	0.27	0.97
83	22FM		72	10	0.99	1.00	1.00
171	42FM	(Kroell <i>et al.</i> 1974)	61	0	0.64	0.37	0.82
177	45FM		64	10	0.20	0.38	0.55
189	53FM		75	3	0.84	0.99	0.79
200	60FM		66	9	0.37	0.28	0.70
MRS04	MRT02	(Bouquet <i>et al.</i> 1994)	57	1	0.32	0.62	0.80
CADVE87	170	(Kent <i>et al.</i> 2004)	75	0	0.04	0.00	0.01
CADVE54	145		54	0	0.00	0.00	0.00
CADVE246	189		79	0	0.05	0.00	0.00
CADVE190	186		58	0	0.00	0.00	0.00
CADVE155	176		85	0	0.29	0.00	0.00
1294	411	(Shaw <i>et al.</i> 2009)	76	5	1.00	1.00	0.84
1295	403		47	16	1.00	0.99	0.44
1358	425		54	10	1.00	1.00	0.61
1359	426		49	8	1.00	0.99	0.51
1360	428		57	5	1.00	1.00	0.67
1378	443		72	7	1.00	1.00	0.82
1379	433		40	8	1.00	0.93	0.29
1380	441		37	2	1.00	0.78	0.29

**Table 6. Contingency tables for DcTHOR, shear stress and ultimate strain**

Prediction	Observed		Prediction	Observed	
	NFR2+	Non injurious		Ultimate strain	NFR2+
DcTHOR and shear stress			Ultimate strain		
NFR2+	12	1	NFR2+	11	3
Non injurious	2	8	Non injurious	3	6

If a risk of 0.5 is taken as threshold to define injury, as done by Forman *et al.* (2012), the number of true positives for both DcTHOR and shear stress is 12 while 11 for ultimate strain, as shown in Table 6. The number of false positives

is one for DcTHOR and shear stress while it is three for ultimate strain. These results, in this particular sample, indicate a better performance in predicting NFR2+ for DcTHOR and shear stress than ultimate strain.

The ROC curve for the DcTHOR, shear stress and ultimate strain are shown in Figure 15. The DcTHOR and shear stress curves are further away than the ultimate strain from the dashed line. The dashed line represents a criterion with random performance. The circles on the curves represent the true positive and false positive rates when the risk is 0.5. The area under the ROC curve for the DcTHOR is 0.849, for the shear stress 0.845 and for the ultimate strain 0.615.

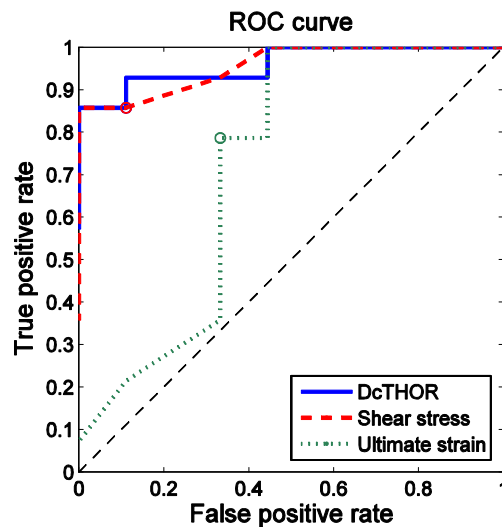


**Figure 15. ROC curve for the DcTHOR, shear stress and ultimate strain criteria**

#### 7.4 Discussion and conclusions

The IRCs for DcTHOR and shear stress classified the injurious and non-injurious tests in a better way than the ultimate strain in the current set of tests. Moreover, the ROC curve indicated a better performance of the DcTHOR and shear stress in the classification of the current set of tests.

As described in Paper II, strain values have a greater variation than stress values once the plastic region is reached, which could explain the fact that IRCs constructed based on strains had greater AIC values (lower AIC values imply a better fit between the IRC and the sample data) and wider confidence intervals than those based on stresses. This phenomenon could also be an explanation for the greater number of false positives and negatives obtained with the ultimate strain compared to those obtained with shear stress.

The material properties in the rib cortical bone differ between the modified THUMS and the THUMS version used by Forman et al. (2012). The modified THUMS referred to in this thesis has an elastic modulus of 13 GPa and a yield stress of 93.5 MPa, while the THUMS in Forman et al. has 10.2 GPa and 65

MPa respectively, while the total number of elements representing the ribs is the same for both models. The influence of these material properties in the classification performance of the injury criteria was not evaluated in this thesis; all simulations have been performed with the modified THUMS.

Even though DcTHOR and shear stress displayed a better classification performance than the ultimate strain, these results are not conclusive since the set of tests used in this comparison was the same as the one used to construct the IRC for the DcTHOR and shear stress. It is recommended that a comparison using a set of tests independent of both methods to compute the injury risks should be performed.

## 8 General discussion

An accident can be studied by identifying its factors and grouping them in different phases and components, as illustrated by the Haddon matrix shown in Table 7 (Haddon 1968). This thesis focuses on the human component in the crash phase. The first aim of the thesis is to assess and in its case improve the biofidelity of an FE-HBM. In this thesis, the biofidelity assessment has been done by comparing the kinematic and dynamic responses of the modified THUMS to those of PMHSs in frontal impact conditions (Paper I). The second aim of the thesis was addressed by constructing and evaluating IRCs for the modified THUMS (Paper II). The evaluation of IRCs was also done by comparing the risks obtained with those IRCs to risks seen in real-world frontal impacts (Paper III). In Section 7 of this thesis the evaluation of IRCs was done by comparing the constructed IRCs to the ultimate strain method (Forman et al. 2012). Finally, the third aim of thesis was addressed by exploring the application of an FE-HBM to aid in the development of an updated ATD (Paper IV). The modified THUMS and thoracic injury risk curves presented in this thesis aim to aid the evaluation and design process of restraint systems in frontal crashes. Improved restraint systems in frontal crashes enhance occupant protection and contribute to the reduction in number and severity of thoracic injuries, which was the general aim of this thesis.

**Table 7. Haddon matrix illustrating the focus of this thesis**

		Components		
		Human	Vehicle	Environment
Phases	Pre-crash	Training Attitudes Experience	Roadworthiness Lighting Braking	Road geometry Road surface Visibility
	Crash	<i>Biofidelity</i> <i>Injury risk curve</i> <i>Assessment of restraints</i>	Occupant restraints Crash protective design	Guard rails
	Post-crash	First Aid Emergency response	Ease of access Fire risk	Rescue facilities Congestion

### 8.1 Biofidelity

The PMHS tests to modify THUMS v3.0, described in Paper I, included individual rib tests and tests with eviscerated, denuded and intact thoraces. Using data at several detail levels, from organ to intact thoraces, to guide the modifications to THUMS v3.0 provided a more robust method to improve its biofidelity as opposed to using only data at the whole body level. A similar

approach was described by Mordaka et al. (2007) during the development of the HUMOS2 model and in (Gayzik et al. 2012) and (Vavalle et al. 2013b) for the GHMBC. By assessing biofidelity at different levels and individual organs, it is less likely that an organ is compensating for the non-biofidelic response of other organs and still providing a biofidelic response for a particular load case. An example of this would be when the low rib stiffness is compensated by stiffer internal organs, although the thoracic stiffness is within the biofidelity requirements. This multi-level approach is important for the development of FE-HBMs.

The biofidelity of the modified THUMS was assessed by simulating a pendulum to the mid-sternum impact test, four table top tests in which the thorax was loaded dynamically and one full frontal sled test (Paper I). The focus of these assessments was on the thoracic kinematics and stiffness. In this way, tests with different loading conditions were used to check the biofidelity of the modified THUMS. From these tests, the impactor test is representative of a hard contact between the occupant and the car interior. The sled test is representative of a belted occupant. The table top tests include some simplifications with respect to a frontal crash. Firstly the inertia of the whole thorax is not loading the restraint systems. Secondly, the boundary condition at the back of the spine differs from a real crash since the back of the PMHSs is supported by the table. Despite these simplifications, the table top tests are tests suitable for the evaluation of the thoracic stiffness under different loading conditions i.e., hub, diagonal belt, double diagonal belt and band, and thus relevant as biofidelity tests. In particular, the band case in the table top tests has been considered as representative of the distributed load an airbag would impose to the thorax. The band case in the table top test has also been used as a representation of an air bag in the biofidelity assessment of other FE-HBMs, as in the THUMS v4.0 (Kitagawa et al. 2013). The sled test used in the biofidelity assessment of the modified THUMS has also been used in the biofidelity assessment of THUMS v4.0 (Kitagawa et al. 2013) and GHMBC (Vavalle et al. 2013a) models.

The biofidelity of the model was not assessed at the material level response at any whole body test, i.e., the stresses or strains in the rib cortical bone were not compared to data from whole body PMHS tests. An indirect way to assess the biofidelity at this level was through the results from the IRCs in Paper II. The critical values of shear stress and first principal strains in the IRCs, i.e., when risk is 50%, were within the values at time of fracture found experimentally for coupons of human rib cortical bone in tensile tests by Kemper et al. (2005), Kemper et al. (2007), and Subit et al. (2011). Song et al. (2009) has compared the strain response of HUMOS2LAB to impactor tests on PMHS instrumented with uniaxial strain gauges on ribs 1 to 10. Additionally to the indirect

assessment of the stress and strain performed on the modified THUMS, future work should consider the use of whole body PMHS tests where the strains have been measured, as in Trosseille et al. (2008).

## **8.2 Rib loads**

The rib response was investigated in Paper I in order to understand the loads present in a rib during a frontal impact. The simulations of whole body tests revealed a complex load superposition in the ribs during the sled tests. In contrast, the simulations of single rib tests in Paper I predominantly registered bending, and the ribs did not present significant out of plane motions. Single rib tests apply only one of the multiple loads a rib is subjected to in frontal impacts. Hence, using single rib tests to investigate injury criteria is limited by this fact. Therefore, single rib tests were not used to construct injury risk curves in Paper II; instead whole body PMHS tests were used.

In Paper II, the IRC for shear stress obtained lower AIC values than IRC for the first principal stress. Based on this finding it was concluded that the shear stress IRC described the PMHS data more appropriately than first principal stress, i.e., the inclusion of all stress components in the IRC was related to a better performance than if just considering one of the components. Furthermore, this finding supports the results obtained in Paper I regarding complex superposition of loads in the ribs during a frontal crash. Song et al. (2011) reported that the strains obtained in simulations with the HUMOS2LAB model were parallel to the rib axis, in contrast to the findings in Paper I. In table top tests with PMHSs instrumented with triaxial strain gauges, (Duma et al. 2005), found that the first principal strain formed an angle to up to 20 degrees with respect to the rib axis; this result supports findings in Paper I.

The poor result obtained for some of the evaluated injury criteria at the structural level may also be related to the superposition of loads. As described in Paper I, the out of plane displacement in the ribs differed between tests and rib levels. Even though the end to end displacement and rib angle change criteria evaluated in Paper II included the out of plane displacements, since both were measured in the space and not only in the rib plane, their IRCs obtained large AIC values and wide confidence intervals. A possible explanation is that, as the out of plane displacement with the tests and rib level, neither end to end displacement nor the rib angle change criteria are able to resolve the superposition of the injury mechanisms related to the variations in out of plane displacements. Further investigations of single rib response to out of plane displacements together with anteroposterior displacements are needed in order to propose a new criterion at the structural level based on these two parameters.

### 8.3 Injury risk curve construction

In Paper II of this thesis, the construction of the IRCs were based on replicating PMHS tests with the modified THUMS, extracting the injury criteria from the model, classifying the PMHS tests as injurious or non-injurious according to the number of fractured ribs reported in the tests, and using the injury criteria values and the injurious/non-injurious classification as input for the survival analysis. This approach was chosen since the well-defined test conditions were preferred over the uncertainty in initial position, acceleration pulse, etc., inherent to real-world data, as presented in Section 4.4. However, a disadvantage of using PMHS tests is that they are more fragile than living humans, as discussed in Papers II and III. No attempt to adjust the injury level in order to account for differences between PMHSs and living humans has been made in this thesis, in contrast to the adjustment adopted in the construction of IRCs for the updated THOR (Davidsson et al. 2014). The adjustment in Davidsson et al. (2014) assumed all PMHSs with NFR5+ as equivalent to a living human who had only sustained a NFR2+ injury. In this thesis, no adjustment was performed since a conservative approach was preferred. It is conservative since the most fragile case, i.e. the PMHS, is defining the IRC to evaluate restraint systems. Furthermore it is unknown if a constant offset of the NFR scale between PMHSs and living humans is independent of the PMHS age at time of death.

The IRCs for DcTHOR and shear stress criteria were the IRCs that best differentiated between injurious and non-injurious tests among the fourteen evaluated criteria in Paper II. Different restraint systems were included in the set of PMHS tests to avoid biasing the IRC to a certain restraint system. Constructing additional IRCs using sub-groups of the PMHS dataset, one for each restraint type, would indicate if the criteria are restraint dependant. However, the limited number of PMHS tests included in the study did not allow this. Davidsson et al. (2014) found that DcTHOR, while measured with an updated THOR, is not restraint dependent after comparing sub-groups representative of distributed, belt and combined loads to the thorax. The shear stress criterion, being a material level criterion, is not expected to be restraint dependent.

As presented in Section 1, age has an effect on the thoracic response and the thoracic injury outcome. The effect of age has been considered in this study by taking age as a covariate in the construction of IRCs. The effect of age has not been considered in the material properties or geometry of the model, i.e., the material properties and geometry of the model do not change according to age. It is known that several bodily changes occur with age, such as changes in the material properties of bones and cartilages, as described in Zioupos and Currey (1998) and Tamura et al. (2005). The ribcage geometry changes affect the

ribcage deformation, as discussed by Gayzik et al. (2008) and Kent et al. (2005b). Implementing those changes in an FE-HBM was, however, outside the scope of this thesis; but should be addressed in the future.

The parametric survival analysis using the Weibull, log-normal and log-logistic distributions was applied to the real-world data to construct an IRC based on real-world data. In this case, the threshold to classify each event as injurious or non-injurious was the presence of thoracic AIS2+ injuries on the driver. The injury criterion was the equivalent barrier speed. An advantage of this approach is that the drivers represent the population that the restraint systems are aimed at protecting, living humans. A disadvantage is that the boundary conditions are not well defined, even if specific selection criteria were used to select the cases to be included in the IRC construction. Examples of these unknown boundary conditions include seat belt position on the driver, their seated posture, the acceleration pulse, among others.

#### **8.4 Risk comparison**

In this thesis, the risks obtained with the modified THUMS and those from the real-world data IRC have been compared. The following paragraphs intend to give a perspective of this comparison.

The data included in the construction of the IRC based on real-world data include the equivalent barrier speed, age and an injury/non-injury classification of the driver for single frontal impacts, as described in Paper III. As discussed in Section 8.3, there are uncertainties in the construction of IRCs based on real-world data. For example, different acceleration pulses could yield the same equivalent barrier speed, as described by (Woolley et al. 2008). An IRC relating equivalent barrier speed to risk of NFR2+ is therefore leaving aside some information from the actual impacts. Different approaches to address the uncertainties in boundary conditions have been proposed. Eriksson et al. (2006) reproduced 110 occupants in real-world rear impacts with known acceleration pulses with an MB-ATD. They performed 100 simulations for reconstructed impact by considering different seat geometries and seated postures, obtaining a range of possible injury criterion for each occupant. In the case of the risk comparisons carried out in Paper III, the available information about the crash severity was the equivalent barrier speed and not the acceleration pulses. Since different acceleration pulses can yield the same equivalent barrier speeds it was identified that an approach similar to the one proposed by Eriksson, et al. would be applied to the simulations of real-world cases in this thesis. In this approach, a set of acceleration pulses yielding a particular equivalent barrier speed could be simulated with the modified THUMS, resulting in a range of injury risk values for a particular speed. This approach was followed in Paper III, but only two acceleration pulses were simulated for each speed. In the case of real-world

crash simulations using FE-HBMs it is not yet practical to perform a very large number of simulations at each equivalent barrier speed, as the method by Eriksson, et al. suggests. Furthermore, the acceleration pulses from the real-world data were not known.

Laituri et al. (2003) simulated frontal car crashes with an MB-ATD in an average car model including variations of acceleration pulse, crash speed and occupant size. Then, based on the real-world frequency of each crash, assigned a weighting factor for the injury risk predicted by the MB-ATD for each simulated crash. Again, since the acceleration pulses were not known in Paper III, it was not possible to assign a real-world frequency to a set of pulses.

The risks predicted with the DcTHOR and shear stress criteria, and the modified THUMS overestimated the risks obtained from the IRC based on real-world data, partly because the fragility of PMHSs. At the same time, these criteria performed best in describing the PMHS data. On the contrary, Dmax criterion predicted risks close to those obtained from real-world data but was not among the two best criteria describing PMHS data. The question of which criterion to use arises, the one that predict risks closer to the real-world data or the one that better describes the PMHS data. Since the real-world data lack some information about the impacts and the modified THUMS will be applied to the evaluation of restraint systems, it is suggested that the criteria that better described PMHS data are to be used. The DcTHOR and shear stress IRCs provided in this thesis are conservative in their rib fracture prediction, but would be suitable when evaluating various frontal restraint system designs.

There were two IRCs that performed similarly in describing the PMHS data. To determine which one to use, it is necessary to study the curves and the results obtained in the sensitivity analysis carried out in Paper II. The shear stress criterion had a much steeper curve than the DcTHOR curve, which could easily lead to sub-optimisation of restraint designs. The shear stress criterion was also more sensitive than DcTHOR to changes introduced to the material properties of the rib cortical bone and changes to restraint position relative to the thorax. The suggestion here would be to use both criteria, but to keep in mind that the shear stress criterion would more easily lead to sub-optimisation. This can be solved by performing simulations where the rib cortical bone material properties are varied.

DcTHOR (Davidsson et al. 2014) was recommended as one of the injury criteria for the updated THOR. This criterion was also found to be the injury criterion at the global level that best predicted injury in the selected PMHS tests and with the modified THUMS. This finding supports the idea that a global criterion that accounts for asymmetry in the thoracic deflection has advantages over a

criterion that measures deflection at only one point to estimate a risk of rib fractures.

### 8.5 Ultimate strain

The comparison in Section 7 between DcTHOR, shear stress and ultimate strain (Forman et al. 2012) indicated that DcTHOR and shear stress performed better than ultimate strain in classifying the injurious and non-injurious tests, in the particular set of PMHS tests presented in Table 5 and using the modified THUMS. Since the PMHS tests in this set were the same as those used in the construction of the DcTHOR and shear stress IRCs, this result is not conclusive. The classification performance of these criteria should be tested in a set of tests independent of those used in the construction of IRCs. However, as discussed in Paper II, strains tend to have greater variations than stresses once the material model is in the plastic region. This fact may also explain the lower performance of ultimate strain in classifying injurious and non-injurious tests in this set of PMHS tests.

A comparison, similar to that in Paper III, was carried out. The risks predicted by the modified THUMS and the ultimate strain criterion (Forman et al. 2012), for three equivalent barrier speeds and two acceleration pulses for each speed, were compared to the real-world data risks. The obtained results are shown in Figure 16, and they clearly indicate that the predicted risks were greater than the real-world data risks. These results are comparable to those obtained in Paper III for the criterion first principal strain, and also presented in Figure 17.

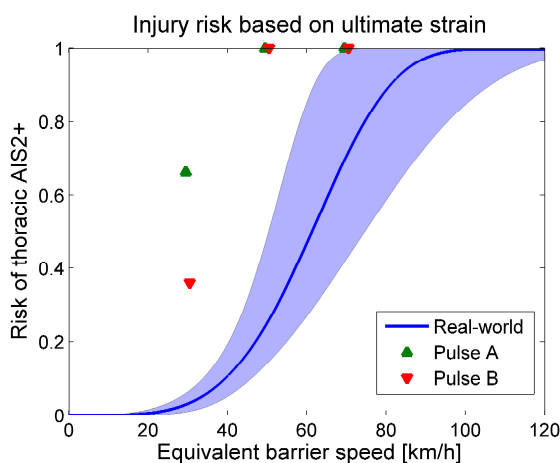


**Figure 16. Risks obtained with the modified THUMS and the ultimate strain criterion**

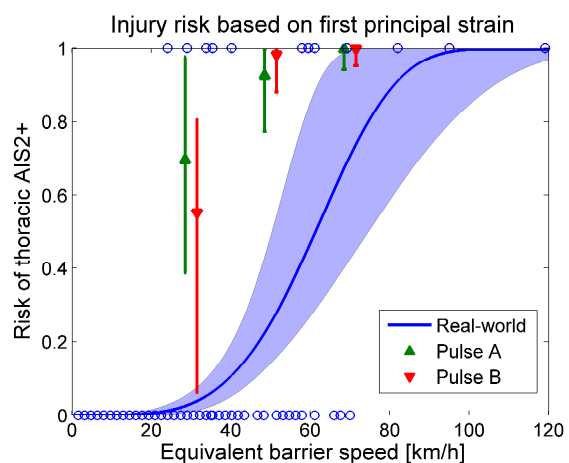


**Figure 17. Risks obtained with the modified THUMS and the first principal strain IRC**

### 8.6 Implications for human body models

An FE-HBM and an injury criterion that can predict rib fractures in several crash directions are tools that have the potential to accelerate and enhance the

design and evaluation of restraint systems. In such cases, a method as the one followed in this thesis can be applied to obtain omnidirectional injury criteria. For the construction of an omnidirectional IRC, an FE-HBM with a biofidelic response in the desired crash directions and a set of PMHS tests covering the desired crash directions would be needed. Then, matched simulations with the FE-HBM and injury outcome from PMHS tests can be used as input for the survival analysis and subsequent construction and evaluation of IRCs. The verification of a common injury mechanism to all included crash directions is particularly important in this case, since different injury mechanisms might be involved in different crash directions. Since a criterion at the global level in a frontal crash is related to the anteroposterior compression of the chest and to the lateral compression in a lateral crash, the criteria at the global level is likely to be associated with different injury mechanisms for the different crash directions. An injury criterion at the material level has better chances than criteria at the structural or global levels of becoming an omnidirectional injury criterion. A material criterion may be related to tension in the rib cortical bone, which could be a common injury mechanism for different crash directions. Effective plastic strain, a material level criterion, has been applied to the study of injury in frontal impacts (Kitagawa et al. 2013) and lateral impacts (Golman et al. 2014).

### **8.7 Future work**

The work in this thesis has been based on a 50<sup>th</sup> percentile male modified THUMS. It is important that future work includes models of different sizes and material properties to avoid sub-optimisation of the restraint systems if they are only designed and optimised to protect a 50<sup>th</sup> percentile male model. One approach to avoid sub-optimisation is to generate models representative of other sizes, as has been done for ATDs, and also including changes in material properties, as described by (Ito et al. 2009) for an FE-HBM. Another potential approach to solve this issue would be to obtain the probabilistic distributions for the factors that affect the risk of rib fractures, such as occupant mass, ribcage geometry, age, gender, and rib cortical bone thickness for the relevant population. When the distributions are known, they are transferred to a parametric FE-HBM to define its geometry and material properties, as presented by Li et al. (2011) for a paediatric head FE model. A set of these parametric models could then be used to estimate the protection offered by a new restraint system for a particular population.

The work in this thesis has focused on frontal impacts, where the number of thoracic injuries is high. A future task is to extend the biofidelity assessment of the model kinematics and thoracic stiffness to oblique and lateral load cases. This task is also a requirement for the generation of omnidirectional FE-HBMs, discussed in Section 8.6.

THUMS v3.0 does not include the models of individual thoracic internal organs. Therefore injuries to the internal thoracic organs have not been directly assessed in this thesis. They have only been indirectly assessed through the presence of rib fractures. Future models should also include the individual description of thoracic internal organs and IRCs for these organs should be constructed.

## 9 Conclusions

Modifications to THUMS v3.0, based on a multi-level approach have been carried out. The biofidelity of the modified THUMS was then assessed in a set of tests representative of loads from frontal car crashes. The contribution of this thesis includes the modifications of THUMS v3.0, the biofidelity assessment of the modified THUMS, with an enhanced biofidelity in frontal impacts compared to THUMS v3.0.

IRCs for the modified THUMS, DcTHOR and shear stress, including age as covariate, to predict the risk of two or more fractured ribs in frontal car crashes have been provided in Paper II of this thesis. These IRCs, together with the modified THUMS, are suitable for being put into immediate use in the industry to evaluate and design restraint systems.

An IRC based on real-world data was constructed and it was found that the DcTHOR and shear stress IRCs predicted risks that were higher than the ones predicted by the real-world IRC. Despite this result, the DcTHOR and shear stress IRCs are suggested to be used with the modified THUMS.

The performance, using the modified THUMS, in classifying NFR2+ and non-injurious tests was compared between the DcTHOR, shear stress, and the ultimate strain method proposed by Forman et al. (2012). DcTHOR and shear stress criteria showed a better performance in classifying the set of tests used in Paper II. A comparison based on a set of tests independent of both methods would be needed to reach a conclusive result.

The modified THUMS was used to support the design of an updated THOR. The first recommendation to improve the THOR's design was to represent the stiffness of the internal organs as spring-damper mechanisms between the spine and ribs and decrease the rib stiffness. The second was to include a textile material to represent the intercostal muscles.

## References

- Akaike, H. (1974). A new look at the statistical model identification. *IEEE Transactions on Automatic Control* 19(6): 716-723.
- Al-Hassani, A., H. Abdulrahman, I. Afifi, et al. (2010). Rib Fracture Patterns Predict Thoracic Chest Wall and Abdominal Solid Organ Injury. *American Surgeon* 76(8): 888-891.
- Association for the Advancement of Automotive Medicine (1998). The Abbreviated Injury Scale-1990 Revision, Update 1998. Des Plaines, IL.
- Battle, C. E., H. Hutchings and P. A. Evans (2012). Risk factors that predict mortality in patients with blunt chest wall trauma: A systematic review and meta-analysis. *Injury-International Journal of the Care of the Injured* 43(1): 8-17.
- Battle, C. E., H. Hutchings and P. A. Evans (2013). Blunt chest wall trauma: a review. *Trauma* 15(2): 156-175.
- Bean, J. D., C. J. Kahane, M. Mynatt, et al. (2009). Fatalities in Frontal Crashes Despite Seat Belts and Air Bags – Review of All CDS Cases – Model and Calendar Years 2000-2007 – 122 Fatalities, Office of Vehicle Safety National Highway Traffic Safety Administration.
- Bose, D., M. Segui-Gomez and J. R. Crandall (2011). Vulnerability of female drivers involved in motor vehicle crashes: an analysis of US population at risk. *Am J Public Health* 101(12): 2368-2373.
- Bouquet, R., M. Ramet and D. Cesari (1994). Thoracic and pelvis human response to impact. International Technical Conference on Enhanced Safety of Vehicles, May 23-26, Munich, Germany.
- Burnham, K. P., D. R. Anderson and K. P. Burnham (2002). Model selection and multimodel inference : a practical information-theoretic approach. New York, Springer.
- Carroll, J. (2009). Matrix of serious thorax injuries by occupant characteristics, impact conditions and restraint type and identification of the important injury mechanisms to be considered in THORAX and THOMO. COVER project GA No. 218740, Deliverable D5-Main summary report.
- Carroll, J., T. Adolph, C. Chauvel, et al. (2010). Overview of serious thorax injuries in European frontal car crash accidents and implications for crash accidents and implications for crash test dummy development. IRCOBI Conference, Sept 15-16. Hanover, Germany: 217-234.
- Carter, D. R. and D. M. Spengler (1978). Mechanical-Properties and Composition of Cortical Bone. *Clinical Orthopaedics and Related Research*(135): 192-217.
- Carter, P. M., C. A. C. Flannagan, M. P. Reed, R. M. Cunningham and J. D. Rupp (2014). Comparing the effects of age, BMI and gender on severe injury (AIS 3+) in motor-vehicle crashes. *Accid Anal Prev* 72(November 2014): 146-160.

- Charpail, E., X. Trosseille, P. Petit, et al. (2005). Characterization of PMHS Ribs: A New Test Methodology. *Stapp Car Crash J* 49: 183-198.
- Cormier, J. M. (2008). The influence of body mass index on thoracic injuries in frontal impacts. *Accident Analysis and Prevention* 40(2): 610-615.
- Crandall, J., R. Kent, J. Patrie, J. Fertile and P. Martin (2000). Rib fracture patterns and radiologic detection--a restraint-based comparison. *Annu Proc Assoc Adv Automot Med* 44: 235-259.
- Cuerden, R., R. Cookson, P. Massie and M. Edwards (2007). A review of the european 40% offset frontal impact test configuration. *International Technical Conference on the Enhanced Safety of Vehicles*, June 18-21 Lyon, France.
- Davidsson, J., J. Carroll, D. Hynd, et al. (2014). Development of injury risk functions for use with the THORAX Demonstrator; an updated THOR. *IRCOBI Conference*, Sept 10-12. Berlin, Germany.
- Duma, S., J. Stitzel, A. Kemper, et al. (2006). Acquiring non-censored rib fracture data during dynamic belt loading. *Biomed Sci Instrum* 42: 148-153.
- Duma, S., J. Stitzel, A. Kemper, et al. (2005). Non-censored rib fracture data from dynamic belt loading tests on the human cadaver thorax. *International Technical Conference on the Enhanced Safety of Vehicles*, June 6-9, Washington, D.C., US.
- Eppinger, R., E. Sun, F. Bandak, et al. (1999). Development of improved injury criteria for the assessment of advanced restraint systems - II, NHTSA.
- Eriksson, L. and A. Kullgren (2006). Influence of seat geometry and seating posture on NIC(max) long-term AIS 1 neck injury predictability. *Traffic Inj Prev* 7(1): 61-69.
- Evans, L. (2001). Female compared with male fatality risk from similar physical impacts. *J Trauma* 50(2): 281-288.
- First Technology Safety Systems (2008). FTSS LS-DYNA model of the Hybrid III 50th percentile male dummy: User manual. Version 7.0.
- Foret-Bruno, J., F. Hartemann, C. Thomas, et al. (1978). Correlation between thoracic lesions and force values measured at the shoulder of 92 belted occupants involved in real accidents. *Stapp Car Crash J* 22: 271-291.
- Forman, J. L. and R. W. Kent (2014). The effect of calcification on the structural mechanics of the costal cartilage. *Computer Methods in Biomechanics and Biomedical Engineering* 17(2): 94-107.
- Forman, J. L., R. W. Kent, K. Mroz, et al. (2012). Predicting rib fracture risk with whole-body finite element models: development and preliminary evaluation of a probabilistic analytical framework. *Ann Adv Automot Med* 56: 109-124.

- Foster, J., J. Kortge and M. Wolanin (1977). Hybrid III - A biomechanically based crash test dummy. *Stapp Car Crash J* 21: 975-1014.
- Gayzik, F. S., D. Moreno, N. Vavalle, A. Rhyne and J. Stitzel (2012). Development of a full human body finite element model for blunt injury prediction utilizing a multy-modality medical imaging protocol. 12th International LS-DYNA Users Conference. Dearborn, Michigan.
- Gayzik, F. S., M. M. Yu, K. A. Danelson, D. E. Slice and J. D. Stitzel (2008). Quantification of age-related shape change of the human rib cage through geometric morphometrics. *Journal of Biomechanics* 41(7): 1545-1554.
- Global Road Safety Facility; The World Bank; Institute for Health Metrics and Evaluation (2014). *Transport for health: the global burden of disease from motorized transport*. Seattle, WA: IHME; Washington, DC: The World Bank.
- Golman, A. J., K. A. Danelson, L. E. Miller and J. D. Stitzel (2014). Injury prediction in a side impact crash using human body model simulation. *Accident Analysis and Prevention* 64: 1-8.
- Gomez, M. A. and A. M. Nahum (2002). *Biomechanics of bone. Accidental injury: biomechanics and prevention*. A. M. Nahum and J. W. Melvin. New York, US, Springer.
- Haddon, W., Jr. (1968). The changing approach to the epidemiology, prevention, and amelioration of trauma: the transition to approaches etiologically rather than descriptively based. *Am J Public Health Nations Health* 58(8): 1431-1438.
- Haddon, W., Jr. (1973). Energy damage and 10 countermeasure strategies. *Journal of Trauma Injury Infection and Critical Care* 13(4): 321-331.
- Haffner, M., R. Eppinger, N. Rangarajan, et al. (2001). Foundations and elements of the NHTSA THOR alpha ATD design. International Technical Conference on the Enhanced Safety of Vehicles, June 4-7, Amsterdam, The Netherlands.
- Hallquist, J. O. (2006). *LS-DYNA Keyword user's manual*. Version 970, Livermore Software Technology Corporation.
- Hertz, E. (1993). A note on the head injury criterion (HIC) as a predictor of the risk of skull fracture. *Ann Adv Automot Med* 37: 303-312.
- Hoffmeister, B. K., S. R. Smith, S. M. Handley and J. Y. Rho (2000). Anisotropy of Young's modulus of human tibial cortical bone. *Med Biol Eng Comput* 38(3): 333-338.
- Holmqvist, K. (2009). *Chest injuries in heavy vehicle frontal collisions - Evaluation and adaptation of the Hybrid III dummy instrumentation and injury reference values by means of Human Body Modeling*. Licentiate, Chalmers University of Technology.
- Horsch, J., J. W. Melvin, D. Viano and H. Mertz (1991). Thoracic injury assessment of belt restraint systems on Hybrid III chest compression. *Stapp Car Crash J* 35: 85-108.

- International Organization for Standardization (ISO) (2014). ISO/TS 18506:2014: Procedure to construct injury risk curves for the evaluation of road user protection in crash tests. Geneva, Switzerland, ISO.
- Ito, O., Y. Dokko and K. Ohashi (2009). Development of Adult and Elderly FE Thorax Skeletal Models.
- Iwamoto, M., Y. Kisanuki, I. Watanabe, et al. (2002). Development of a finite element model of the total human model for safety (THUMS) and application to injury reconstruction. IRCOBI Conference, Sept 18-20. Munich, Germany.
- Karmy-Jones, R. and G. J. Jurkovich (2004). Blunt chest trauma. *Curr Probl Surg* 41(3): 211-380.
- Kemper, A. R., C. McNally, E. A. Kennedy, et al. (2005). Material properties of human rib cortical bone from dynamic tension coupon testing. *Stapp Car Crash J* 49: 199-230.
- Kemper, A. R., C. McNally, C. A. Pullins, et al. (2007). The biomechanics of human ribs: material and structural properties from dynamic tension and bending tests. *Stapp Car Crash J* 51: 235-273.
- Kennedy, E. A., W. J. Hurst, J. D. Stitzel, et al. (2004). Lateral and posterior dynamic bending of the mid-shaft femur: fracture risk curves for the adult population. *Stapp Car Crash J* 48: 27-51.
- Kent, R. (2002). Dynamic response of the thorax: restraint specific hard tissue injury. PhD, University of Virginia.
- Kent, R., B. Henary and F. Matsuoka (2005a). On the fatal crash experience of older drivers. *Annu Proc Assoc Adv Automot Med* 49: 371-391.
- Kent, R., S. H. Lee, K. Darvish, et al. (2005b). Structural and material changes in the aging thorax and their role in crash protection for older occupants. *Stapp Car Crash J* 49: 231-249.
- Kent, R., D. Lessley and C. Sherwood (2004a). Thoracic response to dynamic, non-impact loading from a hub, distributed belt, diagonal belt, and double diagonal belts. *Stapp Car Crash J* 48: 495-519.
- Kent, R., D. Murakami and S. Kobayashi (2005c). Frontal thoracic response to dynamic loading: the role of superficial tissues, viscera and the ribcage. IRCOBI Conference, Sept 21-23. Prague, Czech Republic: 355-365.
- Kent, R. W., J. L. Forman and O. Bostrom (2010). Is There Really a "Cushion Effect"? A Biomechanical Investigation of Crash Injury Mechanisms in the Obese. *Obesity* 18(4): 749-753.
- Kent, R. W. and J. R. Funk (2004b). Data Censoring and Parametric Distribution Assignment in the Development of Injury Risk Functions from Biochemical Data.
- Kimpara, H., M. Iwamoto, I. Watanabe, et al. (2006). Effect of assumed stiffness and mass density on the impact response of the human chest

- using a three-dimensional FE model of the human body. *J Biomech Eng* 128(5): 772-776.
- Kindig, M. (2009). Tolerance to failure and geometric influenced on the stiffness of human ribs under anterior-posterior loading. MSc. in Mechanical Engineering, University of Virginia.
- Kitagawa, Y. and T. Yasuki (2013). Correlation among seatbelt load, chest deflection, rib fracture and internal organ strain in frontal collisions with human body finite element models. IRCOBI Conference, Sept 11-13. Gothenburg, Sweden.
- Kleinbaum, D. G. and M. Klein (2012). *Survival analysis: a self-learning text*, Springer New York.
- Kleinberger, M., E. Sun, R. Eppinger, S. Kuppia and R. Saul (1989). Development of improved injury criteria for the assessment of advanced automotive restraint systems, NHTSA.
- Kleiven, S. (2007). Predictors for traumatic brain injuries evaluated through accident reconstructions. *Stapp Car Crash J* 51: 81-114.
- Kroell, C. K., D. C. Schneider and A. M. Nahum (1974). Impact tolerance and response of the human thorax II. SAE Technical paper Paper No. 741187: 383-457.
- Kuppia, S., J. Wang, M. Haffner and R. Eppinger (2001). Lower extremity injuries and associated injury criteria. International Technical Conference on the Enhanced Safety of Vehicles, June 4-7, Amsterdam, The Netherlands.
- Laituri, T. R., B. P. Kachnowski, P. Prasad, K. Sullivan and P. A. Przybylo (2003). A theoretical, risk assessment procedure for in-position drivers involved in full-engagement frontal impacts. SAE World Congress, Detroit, MI, SAE International.
- Lemmen, P., B. Been, J. Carroll, et al. (2013). An advanced thorax-shoulder design for the THOR dummy. International Technical Conference on the Enhanced Safety of Vehicles, May 27-30, Seoul, Korea.
- Li, Z., M. W. Kindig, J. R. Kerrigan, et al. (2009). Rib fractures under anterior-posterior dynamic loads: experimental and finite-element study. *J Biomech* 43(2): 228-234.
- Li, Z., M. W. Kindig, D. Subit and R. W. Kent (2010). Influence of mesh density, cortical thickness and material properties on human rib fracture prediction. *Med Eng Phys* 32(9): 998-1008.
- Li, Z. G., J. W. Hu, M. P. Reed, et al. (2011). Development, Validation, and Application of a Parametric Pediatric Head Finite Element Model for Impact Simulations. *Annals of Biomedical Engineering* 39(12): 2984-2997.
- Mendoza-Vazquez, M., K. Brodin, J. Davidsson and J. Wismans (2013). Human rib response to different restraint systems in frontal impacts: a study using a human body model. *International Journal of Crashworthiness* 18(5): 516-529.

- Mertz, H., J. Horsch, G. Horn and R. Lowne (1991). Hybrid III sternal deflection associated with thoracic injury severities of occupants restrained with force-limiting shoulder belts. International Congress and Exhibition, Detroit, US, SAE International.
- Mertz, H., P. Prasad and G. Nusholtz (1996). Head injury risk assessment for forehead impacts. SAE International Congress and Exposition, Detroit, MI, SAE International.
- Mertz, H. J. and D. A. Weber (1982). Interpretations of the impact responses of a 3-year-old child dummy relative to child injury potential. International Technical Conference on the Enhanced Safety of Vehicles, November 1-4, Kyoto, Japan.
- Mordaka, J., R. Meijer, L. van Rooij and A. Zmijewska (2007). Validation of a finite element human model for prediction of rib fractures. SAE World Congress, Detroit, Michigan, US.
- Murakami, D., S. Kobayashi, T. Torigaki and R. Kent (2006). Finite element analysis of hard and soft tissue contributions to thoracic response: sensitivity analysis of fluctuations in boundary conditions. *Stapp Car Crash J* 50: 169-189.
- Nahum, A. M., C. W. Gadd, D. C. Schneider and C. K. Kroell (1970). Deflection of the human thorax under sternal impact. International Automobile Safety Conference, Society of Automotive Engineers.
- Neathery, R. (1974). Analysis of chest impact response data and scaled performance recommendations. *Stapp Car Crash J* 18: 459-493.
- Nusholtz, G. and R. Mosier (1999). Consistent threshold estimate for doubly censored biomechanical data. SAE International Congress and Exposition, Detroit, MI, SAE International.
- Oshita, F., K. Omori, Y. Nakahira and K. Miki (2002). Development of a finite element model of the human body. 7th International LS-DYNA user conference. Detroit, US: (3-37)-(33-48).
- Petitjean, A., M. Lebarbe, P. Potier, X. Trosseille and J. P. Lassau (2002). Laboratory Reconstructions of Real World Frontal Crash Configurations using the Hybrid III and THOR Dummies and PMHS. *Stapp Car Crash Journal* 46: 27-54.
- Petitjean, A. and X. Trosseille (2011). Statistical simulations to evaluate the methods of the construction of injury risk curves. *Stapp Car Crash J* 55: 411-440.
- Petitjean, A., X. Trosseille, N. Praxl, D. Hynd and A. Irwin (2012). Injury risk curves for the WorldSID 50th male dummy. *Stapp Car Crash J* 56: 323-347.
- Pipkorn, B. and R. Kent (2011). Validation of a human body thorax model and its use for force, energy and strain analysis in various loading conditions. IRCOBI Conference, Sept 14-16. Krakow, Poland: 210-223.

- Pipkorn, B. and K. Mroz (2009). Validation of a Human Body Model for Frontal Crash and its Use for Chest Injury Prediction. SAE International Journal of Passenger Cars - Mechanical Systems 1(1): 1094-1117.
- R Core Team (2012). R: A language and environment for statistical computing, from <http://www.R-project.org/>.
- Ruan, J., R. El-Jawahri, L. Chai, S. Barbat and P. Prasad (2003). Prediction and analysis of human thoracic impact responses and injuries in cadaver impacts using a full human body finite element model. Stapp Car Crash J 47: 299-321.
- Rudd, R. W., J. D. Bean, C. Cuentas, et al. (2009). A study of the factors affecting fatalities of air bag and belt-restrained occupants in frontal crashes. International Technical Conference on the Enhanced Safety of Vehicles, June 15-18, Stuttgart, Germany.
- Shaw, C. G., D. Lessley, J. Crandall, R. Kent and L. Kitis (2005). Dummy torso response to anterior quasi-static loading. International Technical Conference on the Enhanced Safety of Vehicles, June 6-9 Washington, D.C., US.
- Shaw, C. G., D. Parent, S. Purtsezov, et al. (2009a). Frontal impact PMHS sled tests for FE torso model development. IRCOBI Conference, Sept 9-11. York, UK: 341-356.
- Shaw, G., D. Parent, S. Purtsezov, et al. (2009b). Impact response of restrained PMHS in frontal sled tests: skeletal deformation patterns under seat belt loading. Stapp Car Crash J 53: 1-48.
- Shigeta, K., Y. Kitagawa and T. Yasuki (2009). Development of next generation human FE model capable of organ injury prediction. International Technical Conference on the Enhanced Safety of Vehicles, June 15-18, Stuttgart, Germany.
- Song, E., E. Lecuyer and X. Trosseille (2011). Development of injury criteria for frontal impact using a human body FE model. International Technical Conference on the Enhanced Safety of Vehicles, June 13-16, Washington, DC, US.
- Song, E., X. Trosseille and P. Baudrit (2009). Evaluation of thoracic deflection as an injury criterion for side impact using a finite elements thorax model. Stapp Car Crash J 53: 155-191.
- Stigson, H., A. Kullgren and E. Rosen (2012). Injury risk functions in frontal impacts using data from crash pulse recorders. Ann Adv Automot Med 56: 267-276.
- Subit, D., E. d. P. de Dios, J. Valazquez-Ameijide, C. Arregui-Dalmases and J. Crandall (2011). Tensile material properties of human rib cortical bone under quasi-static and dynamic failure loading and influence of the bone microstructure on failure characteristics. arXiv preprint arXiv:1108.0390.

- Tamura, A., I. Watanabe and K. Miki (2005). Elderly human thoracic FE model development and Validation. International Technical Conference on the Enhanced Safety of Vehicles, June 6-9 Washington, DC, US.
- Therneau, T. (2012). A package for survival analysis in S. Version: 2.37-2, from <http://CRAN-R-project.org/package=survival>.
- Tingvall, C. and N. Haworth (1999). Vision Zero: an ethical approach to safety and mobility. 6th ITE International Conference Road Safety & Traffic Enforcement: Beyond 2000, 6-7 September, Melbourne, Australia.
- Toyota Motor Corporation (2008). User's Guide of Computational Human Model THUMS - AM50 Occupant Model: Version 3.0-080225. Toyota Central Labs Inc.
- Trosseille, X., P. Baudrit, T. Leport and G. Vallancien (2008). Rib cage strain pattern as a function of chest loading configuration. *Stapp Car Crash J* 52: 205-231.
- Turner, C. H. (2006). Bone strength: Current concepts. *Skeletal Development and Remodeling in Health, Disease, and Aging* 1068: 429-446.
- Wanek, S. and J. C. Mayberry (2004). Blunt thoracic trauma: flail chest, pulmonary contusion, and blast injury. *Crit Care Clin* 20(1): 71-81.
- Vavalle, N. A., B. C. Jelen, D. P. Moreno, J. D. Stitzel and F. S. Gayzik (2013a). An Evaluation of Objective Rating Methods for Full-Body Finite Element Model Comparison to PMHS Tests. *Traffic Injury Prevention* 14: S87-S94.
- Vavalle, N. A., D. P. Moreno, A. C. Rhyne, J. D. Stitzel and F. S. Gayzik (2013b). Lateral impact validation of a geometrically accurate full body finite element model for blunt injury prediction. *Ann Biomed Eng* 41(3): 497-512.
- Vawter, D. L., Y. C. Fung and J. B. West (1979). Constitutive Equation of Lung Tissue Elasticity. *Journal of Biomechanical Engineering* 101(1): 38-45.
- Vezi, P. and F. Berthet (2009). Structural characterization of human rib cage behavior under dynamic loading. *Stapp Car Crash J* 53: 93-125.
- Vezi, P. and J. Verriest (2005). Development of a set of numerical human models for safety. International Technical Conference on the Enhanced Safety of Vehicles, June 6-9, Washington, DC, US.
- Viano, D. (1986). Biomechanics of bone and tissue: A review of material properties and failure characteristics. SAE Technical paper Paper No. 861923.
- Viano, D. and A. I. King (2000). Biomechanics of chest and abdomen impact. *The biomedical engineering handbook: second edition*. J. D. Bronzino. Boca Raton, US, CRC Press LLC.

- Wismans, J., R. Happee and J. A. W. van Dommelen (2005). Computational human body models. Iutam Symposium on Impact Biomechanics: From Fundamental Insights to Applications 124: 417-429.
- Vittinghoff, E., D. V. Glidden, S. C. Shiboski and C. E. McCulloch (2005). Regression Methods in Biostatistics Linear, Logistic, Survival, and Repeated Measures Models Preface. Regression Methods in Biostatistics: Vii-+.
- Woolley, R. L. and A. Asay (2008). Crash pulse and DeltaV comparisons in a series of crash tests with similar damage (BEV,EES). SAE International Journal of Passenger Cars - Mechanical Systems 1(1): 60-79.
- World Health Organization (2013). Global status report on road safety 2013: supporting a decade of action. Geneva, Switzerland, World Health Organization.
- Zioupos, P. and J. D. Currey (1998). Changes in the stiffness, strength, and toughness of human cortical bone with age. Bone 22(1): 57-66.

## **Appendix A – Validation of a finite element Volvo V70 interior model**

Authors: Manuel Mendoza-Vazquez (Chalmers), Krystoffer Mroz (Autoliv Research), Merete Östmann (VCC)

Division of work: The validation study was planned jointly by the authors. Experimental crash data and the finite element (FE) model of the car interior were supplied by Östmann. The model was improved and validated by Mroz and Östmann. The validated model together with validation results were delivered to Mendoza-Vazquez. The text was revised by all authors.

### **Introduction**

The interior model of a Volvo V70 has been used in Paper III to simulate six impacts, at three different equivalent barrier speeds and two acceleration pulses for each speed. The aim of this appendix is to show the validation of the interior model.

### **Method**

The vehicle interior model of a Volvo V70, shown in Figure A-1, is an FE model of the car cabin including the driver seat, three point seat belt with two pre-tensioners and load limiter, two stages airbag and collapsible steering column. All simulations were performed with the LS-DYNA (LSTC) solver and post-processed using HyperGraph (Altair). The vehicle interior model has been developed by the Volvo Car Corporation, based on CAD data, the car body was meshed at Volvo Car Corporation and assigned the properties according to material test data. For systems such as airbags, seat belts, seats and the steering wheel, the FE models were developed by their suppliers and verified in component or system testing. The model contains about 520,000 elements, of which 390,000 are shells, 126,000 are solids and the remainder discrete and beam elements.

The model was validated by simulating an experimental crash with a Volvo V70 year model 2009 and a Hybrid III 50<sup>th</sup> percentile male ATD in the driver position. Output data were the seat belt forces and Hybrid III chest, head and pelvis accelerations, and the chest compression.



**Figure A-1. Hybrid III in the vehicle interior model**

In the crash test, the Volvo V70 had an initial velocity of 58 km/h and an acceleration pulse at the tunnel according to Figure A-2 and Figure A-3 for the X and Y directions. In the simulation, the acceleration pulses obtained from the crash test were integrated and input as a prescribed velocity to the floor of the vehicle interior model. In the simulation, the Hybrid III 50<sup>th</sup> percentile male ATD was represented by the Hybrid III 50<sup>th</sup> percentile male model version 7.0a (First Technology Safety Systems 2008).

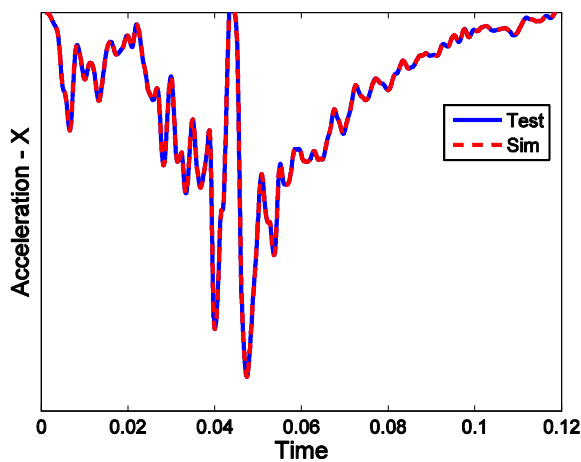


**Figure A-2. Acceleration on X direction**

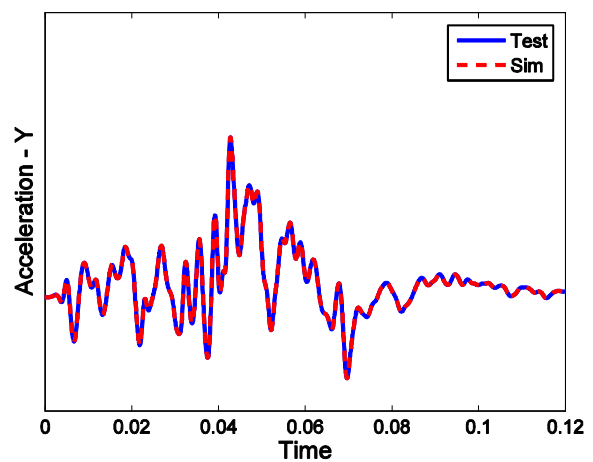


**Figure A-3. Acceleration on Y direction**

## Results

The seat belt forces for the crash test and the simulation are presented in Figure A-4 for the shoulder belt and Figure A-5 for the lap belt on the sill side. The Hybrid III chest compression and resultant acceleration in the test and the simulation are displayed in Figure A-6 and Figure A-7 respectively. The Hybrid III resultant head and pelvis acceleration for the crash test and simulation are presented in Figure A-8 and Figure A-9 respectively. The seat belt forces

measured in the crash test and those calculated in the simulations reach similar levels and have a similar shape. The data obtained with the Hybrid III in the crash test and the simulation also show a good correspondence.

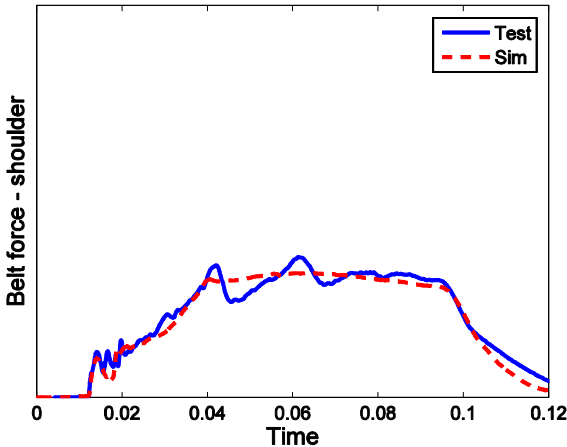


Figure A-4. Shoulder belt force

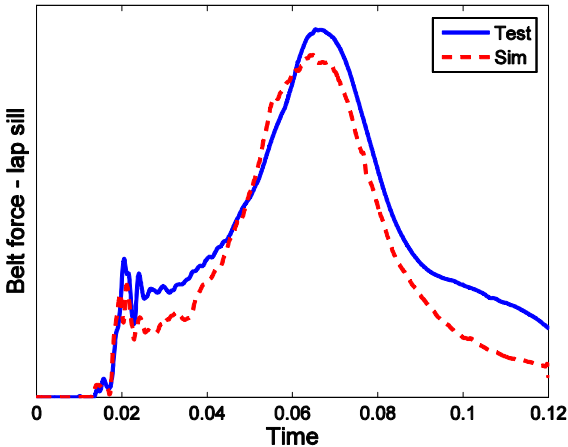


Figure A-5. Lap belt force

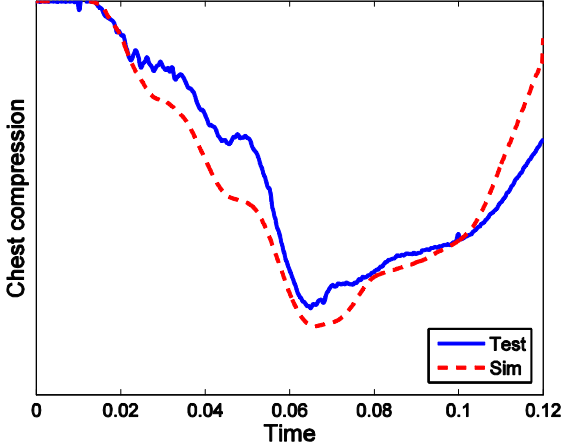


Figure A-6. Hybrid III chest compression

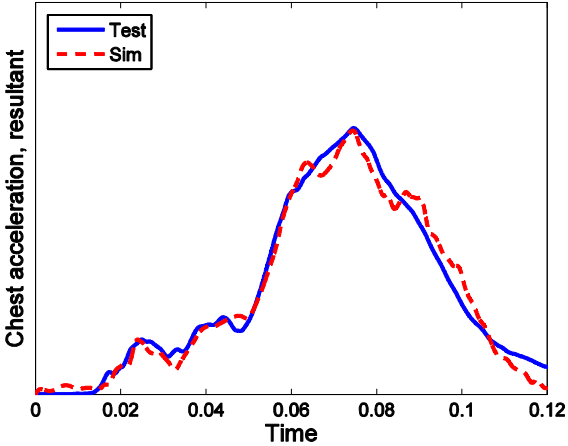


Figure A-7. Hybrid III chest acceleration

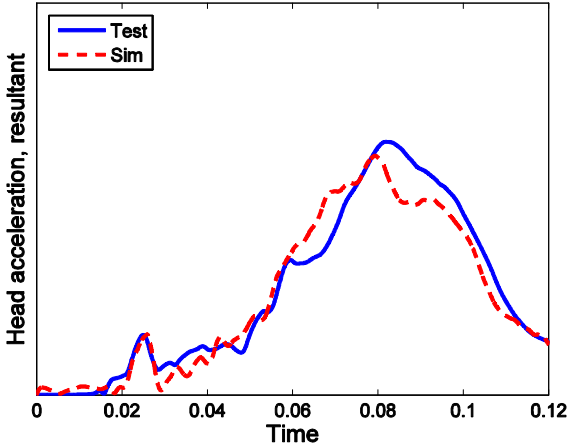


Figure A-8. Hybrid III head acceleration

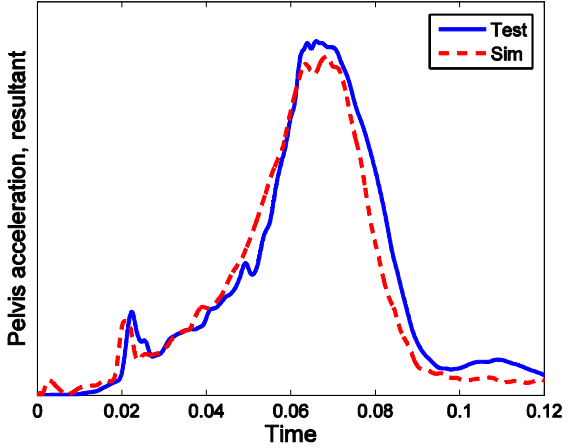


Figure A-9. Hybrid III pelvis acceleration

### **Discussion and conclusions**

As shown in the Results section, the compared signals reached similar levels and have similar shapes. In other words, the interior model decelerated the Hybrid III in the simulation in a comparable way to the deceleration of Hybrid III in the crash test. Since the seat belt forces also coincide between simulation and experiment, the deceleration of the Hybrid III was very likely due to the same components. Thus, the interior model is representative of the interior of a Volvo V70 while restraining a 50<sup>th</sup> percentile Hybrid III.

Despite having considered only one acceleration pulse for this validation, this pulse is comparable to one of the most severe pulses used in the simulations in Paper III. Based on these results, the model is considered adequate in representing the car interior of a Volvo V70 in the six impacts simulated in Paper III.